メラニンの語源と種類

- 語源：ギリシャ語、melanos (“dark”)から由来
- 種類：
  1. Eumelanin (ユー[真正]メラニン)：L-dopaから形成。
  2. Pheomelanin (フェオ[偽]メラニン)：5-S-, 2-S-cysteinyldopa (5S-, 2S-CD)の酸化重合体。
  3. Neuromelanin(神経メラニン)：dopamine, noradrenalinの酸化重合体でこれにcysteninyl基が付加。
  4. Allomelanin(変態メラニン)：通常と異なるメラニン。catechol, 1,8-dihydroxynaphtaleneなどのpolyphenolの酸化物、植物に広く分布し、しばしばNを欠く。

神経冠細胞とメラニン形成

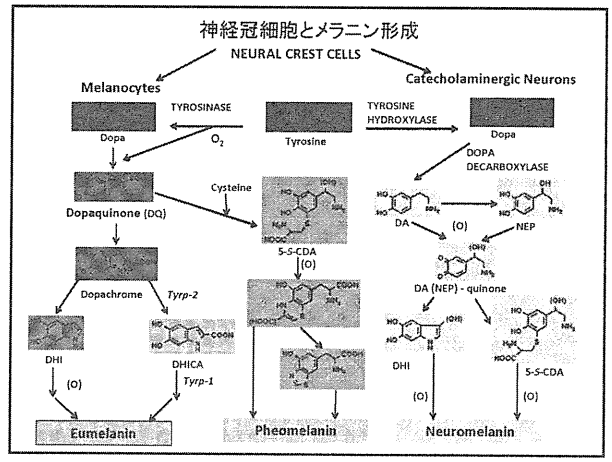

Three Major Distributions of Neuromelanin in Human Brain

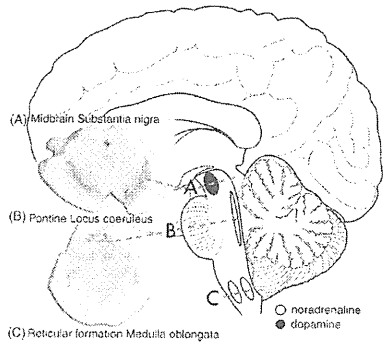

Degradation Products of Neuromelanin by Chemical Reagents

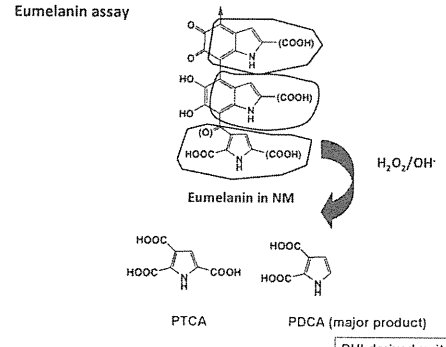

Degradation Products of Neuromelanin by Chemical Reagents

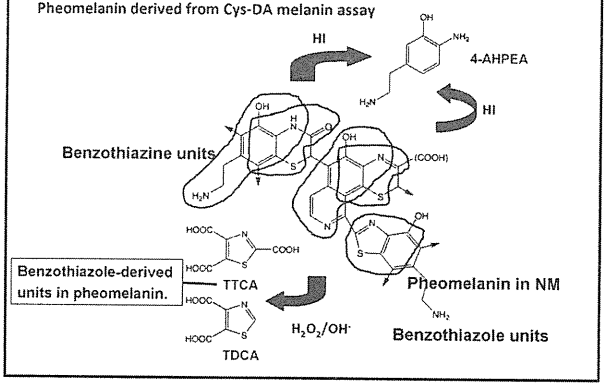

Proposed Model for NM Synthesis in SN Dopaminergic Neurons

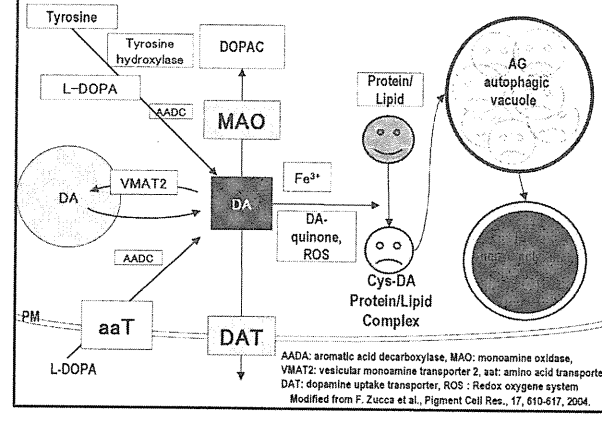

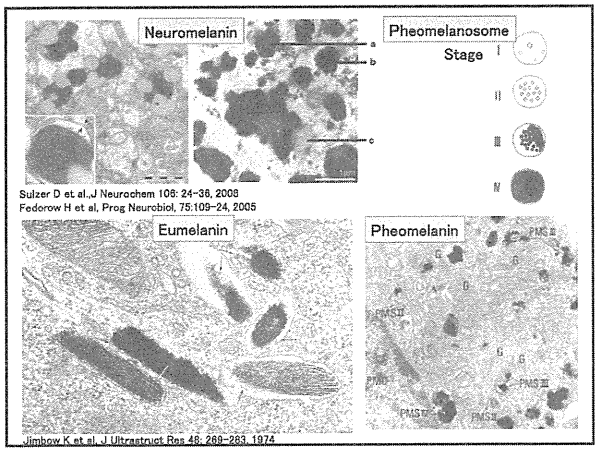
Neuromelanin
Pheomelanosome
Stage
I
II
III
IV
Sulzer D et al.,J Neurochem 106: 24-36, 2008
Fedorow H et al, Prog Neurobiol, 75:109-24, 2005
Eumelanin
Pheomelanin
Jimbow K et al, J Ultrastruct Res 46: 269-283, 1974

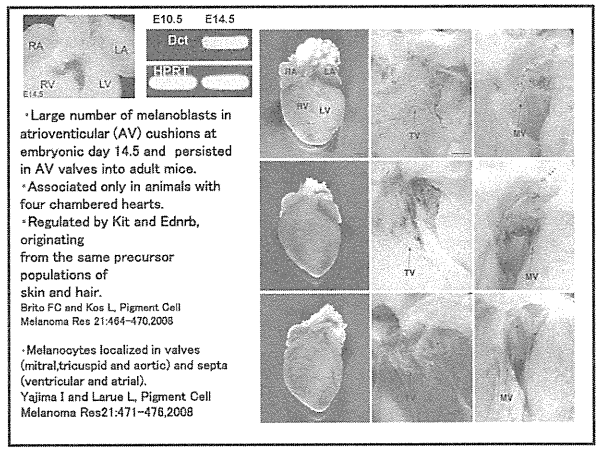
E10.5
E14.5
Dct
Hprt
RA
LA
RV
LV
TV
MV
・Large number of melanoblasts in atrioventicular (AV) cushions at embryonic day 14.5 and persisted in AV valves into adult mice.
・Associated only in animals with four chambered hearts.
・Regulated by Kit and Ednrb, originating from the same precursor populations of skin and hair.
Brito FC and Kos L, Pigment Cell Melanoma Res 21:464-470,2008
・Melanocytes localized in valves (mitral,tricuspid and aortic) and septa (ventricular and atrial).
Yajima I and Larue L, Pigment Cell Melanoma Res21:471-476,2008

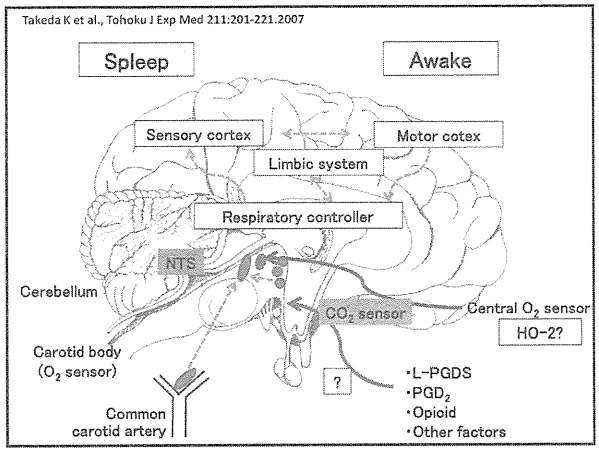
Takeda K et al., Tohoku J Exp Med 211:201-221.2007
Spleep
Awake
Sensory cortex
Motor cotex
Limbic system
Respiratory controller
NTS
Cerebellum
CO2 sensor
Central O2 sensor
HO-2?
Carotid body
(O2 sensor)
Common carotid artery
?
・L-PGDS
・PGD2
・Opioid
・Other factors

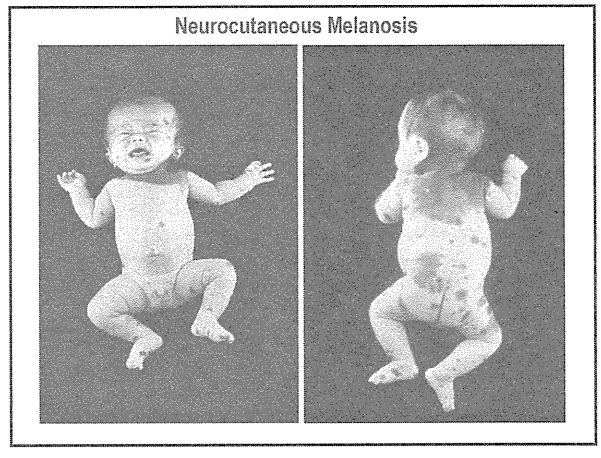
Neurocutaneous Melanosis

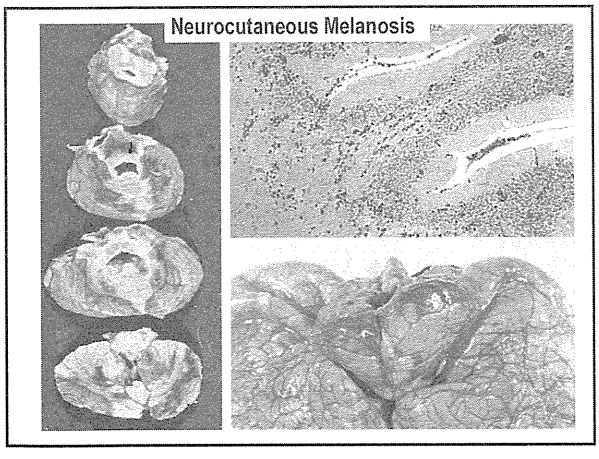
Neurocutaneous Melanosis

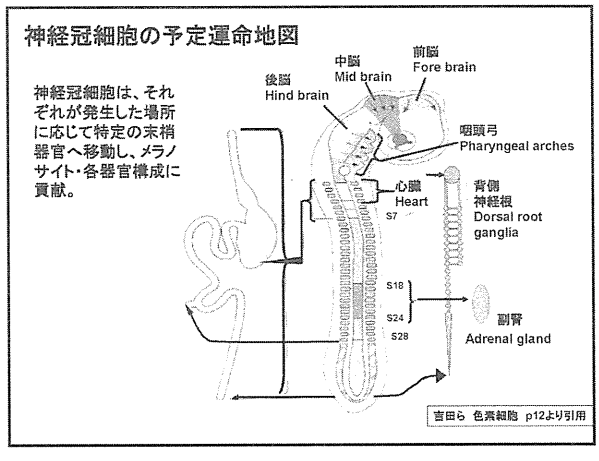
神経冠細胞の予定運命地図
神経冠細胞は、それぞれが発生した場所に応じて特定の末梢器官へ移動し、メラノサイト・各器官構成に貢献。
中脳
Mid brain
前脳
Fore brain
後脳
Hind brain
咽頭弓
Pharyngeal arches
心臓
Heart
S7
背側
神経根
Dorsal root ganglia
S18
S24
S28
副腎
Adrenal gland
吉田ら 色素細胞 p12より引用

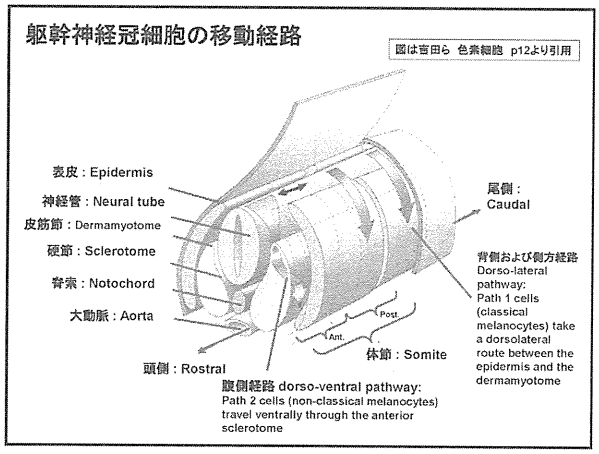
躯幹神経冠細胞の移動経路
図は吉田ら 色素細胞 p12より引用
表皮：Epidermis
神経管：Neural tube
皮筋節：Dermamyotome
硬節：Sclerotome
脊索：Notochord
大動脈：Aorta
尾側：Caudal
背側および側方経路 Dorso-lateral pathway: Path 1 cells (classical melanocytes) take a dorsolateral route between the epidermis and the dermamyotome
Post
Ant.
体節：Somite
頭側：Rostral
腹側経路 dorso-ventral pathway: Path 2 cells (non-classical melanocytes) travel ventrally through the anterior sclerotome

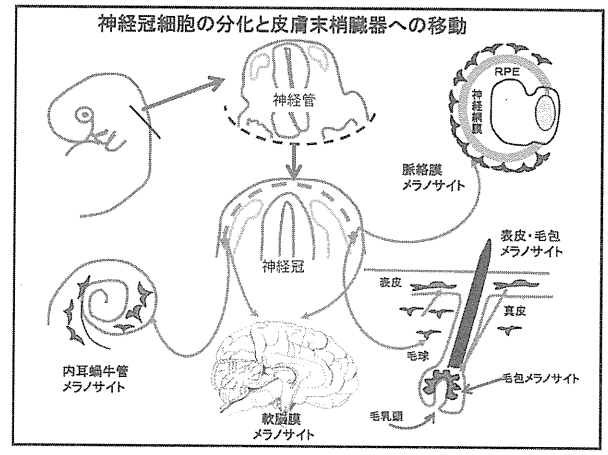
神経冠細胞の分化と皮膚末梢臓器への移動
神経管
RPE
神経網膜
脈絡膜メラノサイト
神経冠
表皮・毛包メラノサイト
表皮
真皮
毛球
毛包メラノサイト
毛乳頭
内耳蝸牛管メラノサイト
軟膜膜メラノサイト

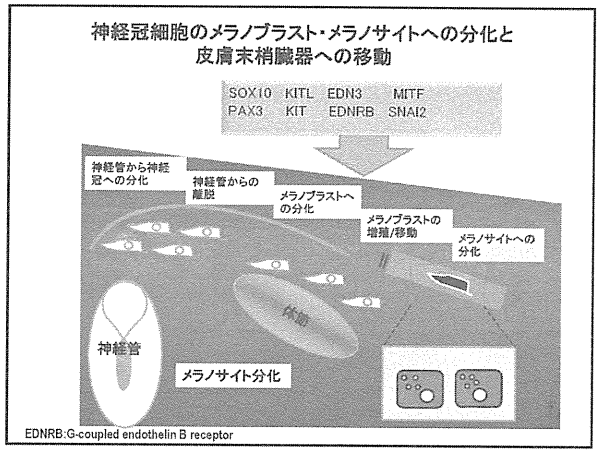
神経冠細胞のメラノブラスト・メラノサイトへの分化と皮膚末梢臓器への移動
SOX10 KITL EDN3 MITF
PAX3 KIT EDNRB SNAI2
神経管から神経冠への分化
神経管からの離脱
メラノブラストへの分化
メラノブラストの増殖/移動
メラノサイトへの分化
体節
神経管
メラノサイト分化
EDNRB:G-coupled endothelin B receptor

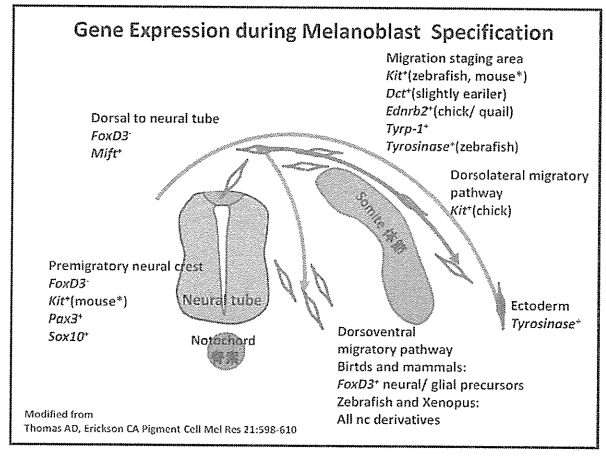
Gene Expression during Melanoblast Specification
Migration staging area
Kit+(zebrafish, mouse*)
Dct+(slightly earlier)
Ednrb2+(chick/ quail)
Tyrp-1+
Tyrosinase+(zebrafish)
Dorsal to neural tube
FoxD3-
Mift+
Dorsolateral migratory pathway
Kit+(chick)
Somite 体節
Premigratory neural crest
FoxD3-
Kit+(mouse*)
Pax3+
Sox10+
Neural tube
Notochord
脊索
Ectoderm
Tyrosinase+
Dorsoventral migratory pathway
Birtds and mammals:
FoxD3+ neural/ glial precursors
Zebrafish and Xenopus:
All nc derivatives
Modified from
Thomas AD, Erickson CA Pigment Cell Mel Res 21:598-610

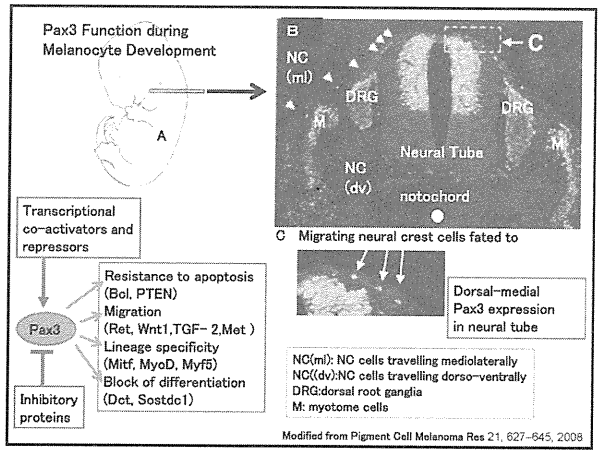
Pax3 Function during Melanocyte Development
A
B
C
NC (ml)
DRG
M
Neural Tube
NC (dv)
notochord
C Migrating neural crest cells fated to
Dorsal-medial Pax3 expression in neural tube
Transcriptional co-activators and repressors
Pax3
Resistance to apoptosis (Bcl, PTEN)
Migration (Ret, Wnt1,TGF- 2,Met)
Lineage specificity (Mitf, MyoD, Myf5)
Block of differentiation (Dct, Sostdc1)
Inhibitory proteins
NC(ml): NC cells travelling mediolaterally
NC((dv):NC cells travelling dorso-ventrally
DRG:dorsal root ganglia
M: myotome cells
Modified from Pigment Cell Melanoma Res 21, 627–645, 2008

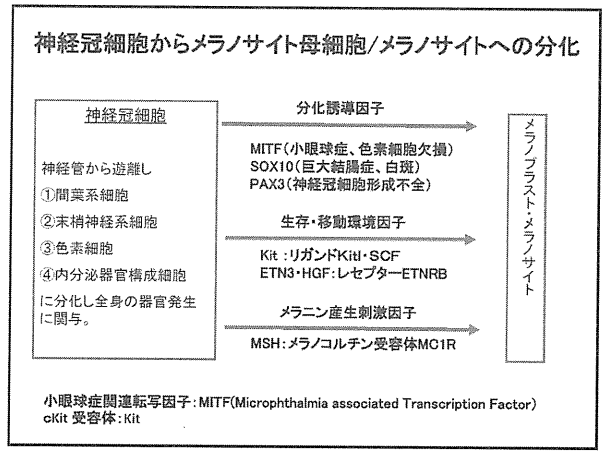
神経冠細胞からメラノサイト母細胞/メラノサイトへの分化
神経冠細胞
神経管から遊離し
①間葉系細胞
②末梢神経系細胞
③色素細胞
④内分泌器官構成細胞
に分化し全身の器官発生に関与。
分化誘導因子
MITF(小眼球症、色素細胞欠損)
SOX10(巨大結腸症、白斑)
PAX3(神経冠細胞形成不全)
生存・移動環境因子
Kit :リガンドKitl・SCF
ETN3・HGF:レセプターETNRB
メラニン産生刺激因子
MSH:メラノコルチン受容体MC1R
メラノブラスト・メラノサイト
小眼球症関連転写因子:MITF(Microphthalmia associated Transcription Factor)
cKit 受容体:Kit

小眼球関連転写因子
(Microphthalmia-Associated Transcription Factor)

- ネズミにおけるMitf locusの変異; 色素脱失, 小眼球, 第二次骨吸収の障害, マスト細胞数減少、早期聾唖
- ヒトにおけMITF locusの変異; Waardenburg syndrome (II)

Waardenburg(WS)症候群
- 知覚神経性先天性難聴、虹彩異色症
- 皮膚毛髪の色素異常(脱失)、
- 内眼角・涙点の外側方偏位、　　鼻根部の肥大

- 遺伝子変異型:
  WS I: PAX3　　WSII: MITF
  WSIII: PAX3　　WSIV:SOX10

まだら症 (Piebaldism)

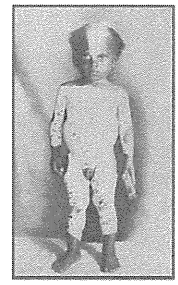

1. KIT遺伝子のキナーゼドメインでの変異によるメラノサイトの胎生期死亡
2. 常染色体優性遺伝
3. 全額部毛髪生え際の三角形の白斑と白毛 (85%)
4. 四肢、躯幹、前胸部の左右対称性白斑
5. 白斑部内の島嶼状配列をとる色素沈着斑

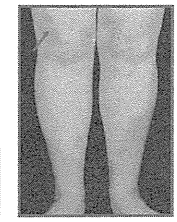

白斑部にはメラノサイトは存在しない。色素沈着部ではメラノサイトが存在し、これらメラノサイトは類円形、細下粒状のメラノソームを産生し、これらメラノソームは角化細胞に受け渡され異常な崩壊を受ける

KIT蛋白突然変異とまだら症及び関連疾患

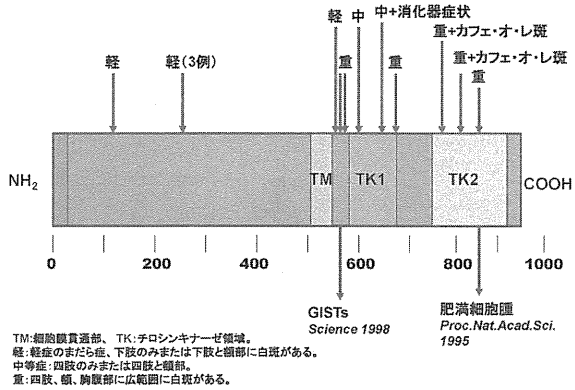

TM:細胞膜貫通部、 TK:チロシンキナーゼ領域。
軽:軽症のまだら症、下肢のみまたは下肢と顔部に白斑がある。
中等症:四肢のみまたは四肢と顔部。
重:四肢、顔、胸腹部に広範囲に白斑がある。

メラノコルチン・ペプチド, POMC, MSH, ACTH

MSH:メラノサイト刺激ホルモン (melanotropin); 脳下垂体; Shizume, Lerner, Fitzpatrick Endocrinology 54:553-560,1954

ACTH:副腎皮質ホルモン (corticotropin); 副腎皮質; Bell PH J Am Chem Soc 76:5565-5567,1954, Riniker et al, Nature 235:114-115, 1972

POMC:proopiomelanocortin, POM(proopiomelanotropin; MSH-A+MSH-B) + POC (proopiocortin;ACTH);Nakanishi et al, Nature 278:5160-5164,1979

メラノコルチンmelanocortin (MC)
- ACTH/MSH由来のペプタイドの総称
- 多くの規制因子とリセプターを介し中枢神経系と多種類の末梢臓器で異なった病的・生理的作用・状態を発現

ヒト POMC:proopiomelanocortin

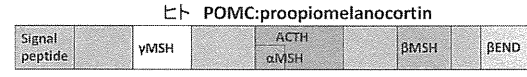

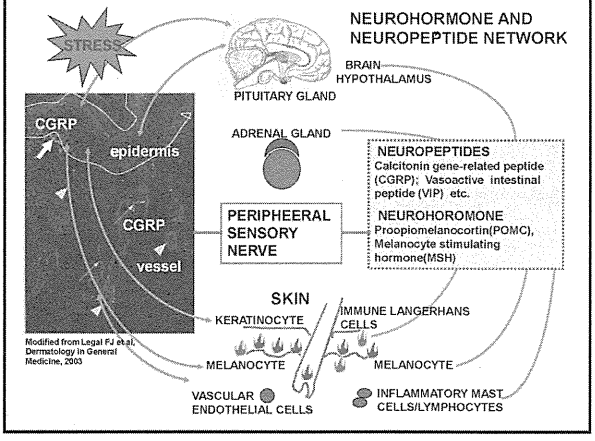

Casing Model of Mixed Melanogenesis for Aging and Antiaging Process

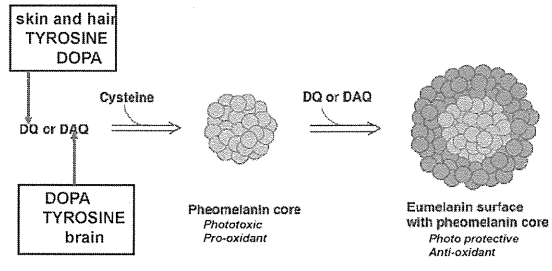

During the process of mixed melanogenesis in human brain and skin, pheomelanic pigment is produced first, followed by deposit of eumelanic pigment. In the granule with the eumelanin surface. This figure is intentionally cut away to reveal the inner pheomelanic core.

Structure and Distribution of Neuromelanin

Characteristics		Neuromelanin
Appearance	Light microscopy	Dark brown to black under visible light Non-fluorescent under UV light
	Electron microscopy	Irregularly shaped granules of varying electron density and size (0.5–2.5 μm) Cytoplasmic Presence or absence of a surrounding membrane is unclear Present at opposing end of neuron to nucleus
Distribution	Human brain	Selected catecholamine neurons only
Development	Temporal pattern	First appearance around 3 years of age Progressively increases over lifespan
Chemistry	Structure	Organic polymer of dopamine metabolic products, 5–15% proteins and one-third lipids by mass Bind a range of functionally active ions, including iron and exotoxins

Biological Roles of Neuromelanin in Human Brain

Characteristics	Neuromelanin
Formation and degradation	No enzymatic regulation mechanism identified Non-degraded *in vivo*; released from dying neurons and removed from brain via immune pathways
Functional roles in health and diseases	May inactivate cellular metabolites and cations, in particular iron Possible role as a free radical scavenger May function as an intracellular iron regulatory system Changes in neuromelanin may underlie cell vulnerability in Parkinson's diseases

Comparison of Species, Organs and Cells between Skin Melanin and Neuromelanin

Characteristic		Melanin	Neuromelanin
Occurrence and Distribution of pigment	Species	Vertebrates	●Primates, greatest amount in humans
	Organs specifically within humans	Hair, skin, iris and choroid of eye, inner ear; Retinal pigment epithelium	●Not found in common laboratory animals, e.g., rat ●Selected catecholamine neurons, predominantly substantia nigra and locus coeruleus of the midbrain
	Organs not identified in humans	Heart, Adipose tissue Lung	N/A Neurons
Cells that produce pigment		Melanocytes	

Comparison in Organelles and Maturation of Skin Melanin and Neuromelanin

Characteristic		Melanin	Neuromelanin
Organelles	Ultrastructure	●Discrete membrane-bound melanosomes Spherical or ellipsoidal in shape	●Indistinctly bordered granules, not membrane-bound, wide size range ●Three main components: Dense pigment, lucent lipid & protein
	Maturation	●Internal structure of melanosome visible at first but gradually obscured by deposited melanin in eumelanosomes ●Structure remains visible in pheomelanosomes	Unknown

Comparison in Pigment Genesis and Degradation of Skin Melanin and Neuromelanin

Characteristic		Melanin	Neuromelanin
Regulation of pigment genesis	Genetic Cellular	Regulation by 85 distinct gene loci Hormonally regulated by MCIR agonists MSH and ASP	Unknown Unknown
	Within Melanosome/ granule	●Rate limiting enzyme, tyrosinase,TYRP,DCT ●pH of melanosome	●TH, other enzyme currently not identified ●Effect of pH unknown
Cells that contain pigment		Melanocytes, Keratinocytes	Neurons, occasional glial cells
Degradation			Released from dying neurons in PD, catabolism unknown ●Catabolism in healthy brain not investigated

Comparison in Structure and Biological Roles of Skin Melanin and Neuromelanin

Characteristic	Melanin	Neuromelanin
Chemical structure	●Heterologous polymer, basic structural unit generally represented by covalently linked indoles	●Complex heterologous polymer similar to melanin
Biological role in humans	●Integral protein component ●Ocular development ●Photoprotective ●Binding of iron and other metals ●Inner ear-maintenance of ionic composition of endolymph ●Absorption of electrons (antioxidant), Neuroendocrine ●Redox properties-antibiotic, metal binding	●Interaction with pesticides, toxins and neuroleptics
Biological role in non-humans	●Respiration regulation ●Atrioventricular development from endocardial cushions in heart	●N/A

Contents lists available at SciVerse ScienceDirect

Journal of Dermatological Science

journal homepage: www.elsevier.com/jds

N-propionyl-4-*S*-cysteaminylphenol induces apoptosis in B16F1 cells and mediates tumor-specific T-cell immune responses in a mouse melanoma model

Yasue Ishii-Osai [a], Toshiharu Yamashita [a,*], Yasuaki Tamura [b], Noriyuki Sato [b], Akira Ito [c], Hiroyuki Honda [d], Kazumasa Wakamatsu [e], Shosuke Ito [e], Eiichi Nakayama [f], Masae Okura [a], Kowichi Jimbow [a]

[a] *Department of Dermatology, Sapporo Medical University School of Medicine, Sapporo 060-8543, Japan*
[b] *First Department of Pathology, Sapporo Medical University School of Medicine, Sapporo 060-8556, Japan*
[c] *Department of Chemical Engineering, Faculty of Engineering, Kyushu University, Fukuoka 819-0395, Japan*
[d] *Department of Biotechnology, School of Engineering, Nagoya University, Nagoya 464-8603, Japan*
[e] *Department of Chemistry, Fujita Health University School of Health Sciences, Toyoake 470-1192, Japan*
[f] *Faculty of Health and Welfare, Kawasaki University of Medical Welfare, Kurashiki 701-0193, Japan*

ARTICLE INFO

Article history:
Received 29 November 2011
Received in revised form 19 April 2012
Accepted 20 April 2012

Keywords:
N-propionyl-4-*S*-cysteaminylphenol
Melanogenesis
Apoptosis
Reactive oxygen species
Tumor suppression
Tyrosinase-related protein

ABSTRACT

Background: N-propionyl-4-*S*-cysteaminylphenol (NPr-4-*S*-CAP) is selectively incorporated into melanoma cells and degrades them. However, it remains unclear whether NPr-4-*S*-CAP can induce cell death associated with the induction of host immune responses and tumor suppression in vivo.
Objective: To examine the molecular mechanism of NPr-4-*S*-CAP-mediated cytotoxicity toward melanoma cells and to test whether NPr-4-*S*-CAP can suppress transplanted primary and secondary B16F1 melanomas.
Methods: Cytotoxicity and apoptosis of melanoma cells were assessed by cell counting, flow cytometry, and detection of reactive oxygen species (ROS) and apoptotic molecules. NPr-4-*S*-CAP-associated host immunity was studied using a B16F1 mouse melanoma model through the application of CD4- and CD8-specific antibodies and tetramer assay.
Results: NPr-4-*S*-CAP suppressed growth of pigmented melanoma cells associated with an increase of intracellular ROS, activation of caspase 3 and DNA fragmentation, suggesting that NPr-4-*S*-CAP mediated ROS production, eliciting apoptosis of melanoma cells. Growth of transplanted B16F1 melanomas was inhibited after the consecutive intratumoral injections of NPr-4-*S*-CAP, and the tumor growth after rechallenge with B16F1 was significantly suppressed in the treated mice. This suppression occurred when the treated mice were given the anti-CD4 antibody, but not the anti-CD8 antibody. Tetramer assay demonstrated increased TYRP-2-specific $CD8^+$ T cells in the lymph node and spleen cells prepared from NPr-4-*S*-CAP-treated B16F1-bearing mice.
Conclusions: These suggest that NPr-4-*S*-CAP induces apoptosis in melanoma cells through ROS production and generates $CD8^+$ cell immunity resulting in the suppression of rechallenge B16F1 melanoma.

1. Introduction

Although early lesions of primary melanoma are curable by excision, treatment of metastatic melanoma is significantly more difficult and the current systemic therapies have little effect on the overall survival rate or period [1,2]. Melanin pigment is synthesized in cytoplasmic organelles called melanosomes, specifically present in differentiated melanocytes. Melanin precursors possess strong cytotoxicity toward various kinds of cells, including melanoma cells, when tyrosinase, a key enzyme of melanin biogenesis, is ectopically expressed [3]. Thus, therapy targeting melanogenesis and enhancing cytotoxicity can be highly effective for growth suppression and possible induction of systemic immune responses against malignant melanoma without significant systemic side effects.

We have employed chemical agents biologically unique to melanoma cells such as the sulfur-amine analogs of tyrosine,

Abbreviations: NPr-4-*S*-CAP, N-propionyl-4-*S*-cysteaminylphenol; NPr-2-*S*-CAP, N-propionyl-2-*S*-cysteaminylphenol; AMF, alternating magnetic field; ROS, reactive oxygen species; TRAIL, tumor necrosis factor-related apoptosis-inducing ligand; DMEM, Dulbecco's modified Eagle's medium; FBS, fetal bovine serum; RPMI, RPMI1640 medium; PBS, phosphate-buffered saline; HSP, heat shock protein; TYRP-1, tyrosinase-related protein-1; TYRP-2, tyrosinase-related protein-2.

* Corresponding author. Tel.: +81 11 611 2111; fax: +81 11 613 3739.
E-mail address: yamasita@sapmed.ac.jp (T. Yamashita).

0923-1811/$36.00 © 2012 Published by Elsevier Ireland Ltd on behalf of Japanese Society for Investigative Dermatology.
http://dx.doi.org/10.1016/j.jdermsci.2012.04.009

N-acetyl-4-*S*-cysteaminylphenol (NAc-4-*S*-CAP) and N-propionyl-4-*S*-cysteaminylphenol (NPr-4-*S*-CAP). They have been shown to be good substrates for tyrosinase [4–6] and to be selectively incorporated into melanoma cells, causing cytotoxicity against them and melanocytes [7–11]. However, it remains unclear whether NPr-4-*S*-CAP can induce cell death associated with the induction of host immune responses resulting in the tumor suppression in vivo.

In this study, we examined the molecular mechanism of NPr-4-*S*-CAP-mediated cytotoxicity toward melanoma cells by focusing on intracellular reactive oxygen species (ROS) and tested whether NPr-4-*S*-CAP could suppress transplanted primary and secondary B16F1 melanomas. We analyzed the molecular basis of B16F1-specific host immunity through the application of CD4- and CD8-specific antibodies. The relations between apoptosis of melanoma cells and ROS production by NPr-4-*S*-CAP and clinical implications for melanoma therapy with this compound are discussed.

2. Materials and methods

2.1. Cell lines and culture

Murine fibroblast NIH3T3, murine melanoma B16F1, human pigmented melanoma 70W and G361, human non-pigmented melanoma TXM18 and SK-mel-24 cell lines were cultured in Dulbecco's modified Eagle's medium (DMEM, Gibco BRL, Gaithersburg, MD, USA) supplemented with 5% fetal bovine serum (FBS) [12]. Human pigmented melanoma cell line M-1 was established from a surgical specimen of a Japanese patient [13] and maintained in RPMI1640 medium (RPMI, Gibco BRL) supplemented with 5% FBS. Murine lymphoma cell line RMA was cultured in RPMI1640 medium supplemented with 5% FBS [12]. Cells were incubated at 37 °C in a 5% CO_2 atmosphere.

2.2. Chemicals

NPr-4-*S*-CAP (MW = 225 Da) was kindly provided by Alberta University's Department of Dermatology (Canada). The compound was synthesized as described by Tandon et al. [9]. NPr-2-*S*-CAP, an inactive form of cysteaminylphenol used as a negative control [5], was synthesized as follows: 195 mg of 2-*S*-cysteaminylphenol, which was prepared by the reaction of phenol with cystamine in 47% HBr [14], was reacted with 1.5 ml of pyridine and 1 ml of propionic anhydride for 30 min at room temperature. After evaporation of the reaction mixture under reduced pressure in a vacuum pump, colorless crystals of NPr-2-*S*-CAP were obtained in a quantitative yield. For the study, NPr-4-*S*-CAP and NPr-2-*S*-CAP were dissolved in propylene glycol (Wako, Osaka, Japan) at a concentration of 244 mM and sterilized by filtration.

2.3. Animal models for tumor formation

Female C57BL/6J mice (4 weeks old, approximately 10.0 g) were obtained from Hokudo (Sapporo, Japan). For the experiment, 3.0×10^5 B16F1 melanoma cells in 0.1 ml of phosphate-buffered saline (PBS) were injected subcutaneously into the right flank in C57BL/6J mice on day 0. On day 8, 24 mice were randomly divided into four treatment groups. From the 8th day, tumor-bearing mice were injected with 0.1 ml of NPr-4-*S*-CAP (24.4 mmol, 5.5 mg) in propylene glycol directly into the tumor with a 26-gauge microsyringe. Group I mice received s.c. administration of NPr-4-*S*-CAP every other day for a total of three days (days 8, 10, and 12) and administration of 0.1 ml of propylene glycol on days 14 and 16. Group II mice received NPr-4-*S*-CAP every other day for a total of five days (days 8, 10, 12, 14, and 16), and in group III NPr-4-*S*-CAP was administered every day for five days (from day 8 to day 12). Control mice were injected with 0.1 ml of propylene glycol every day for five days (Protocol 1). To compare the anti-melanoma effect of NPr-4-*S*-CAP with that of NPr-2-*S*-CAP, mice were divided into another three groups on day 8, and injected with 0.1 ml of NPr-4-*S*-CAP, NPr-2-*S*-CAP or propylene glycol every day for five days (Protocol 2). RMA lymphoma cells (5.0×10^5) were injected subcutaneously into the right flank on day 0 as a control for B16F1 melanoma and, from day 8, mice received NPr-4-*S*-CAP or propylene glycol every day for five days (Protocol 3). Tumor diameters were measured every other day and tumor volumes were calculated using the following formula: long axis × (short axis)^2 × 0.5. The right tumors of treatment and control groups in Protocol 1 were resected surgically on day 22. On day 36, mice were rechallenged with 1.5×10^5 B16F1 cells that were injected into the left flank and tumor diameters were measured every other day from the 37th to 120th days. As a control for B16F1 rechallenge, 2.5×10^5 RMA lymphoma cells in 0.1 ml of PBS were injected subcutaneously into the left flank in group III on day 36.

Animal experiments were carried out according to the principles described in the "Fundamental Guidelines for Proper Conduct of Animal Experiments and Related Activities in Academic Research Institutions under the jurisdiction of the Ministry of Education, Culture, Sports, Science and Technology" of Japan.

2.4. Histopathological study of tumor sections

The tumors were removed and fixed in 10% formalin in PBS. Paraffin-embedded sections were then prepared and processed for hematoxylin–eosin (HE)-staining. For immunohistochemical analysis, the frozen tissues were stained with anti-mouse CD4 mAb (Santa Cruz Biotechnology, Santa Cruz, CA, USA) or anti-mouse CD8 mAb (Acris Antibodies, ACR, Herford, Germany).

2.5. In vivo T-cell depletion assay

Mice that received NPr-4-*S*-CAP every day for five days Protocol 1 were injected with 0.2 mg of an anti-CD4 antibody (anti-mouse CD4, eBioscience, San Diego, CA, USA), anti-CD8 antibody (anti-mouse CD8, eBioscience) or rat IgG (Rat IgG1, aBd Serotec, Kidlington, UK) i.p. on days 29 and 43, i.e., one week before and after the rechallenge test on day 36. The growing tumor diameters were measured and tumor volumes were calculated.

2.6. In vitro cytotoxicity assay

After mice were treated with NPr-4-*S*-CAP every day for five times as described above, the spleen cells were harvested from a mouse which was completely cured by day 36 by NPr-4-*S*-CAP. 5×10^6 spleen cells were then re-stimulated with irradiated B16F1 cells in 2 ml of RPMI1640 supplemented with 50 μM β-mercaptoethanol (Invitrogen, Carlsbad, CA, USA) and 5% FBS for five days. For the control, spleen cells were prepared from a naïve mouse and a mouse transplanted with RMA lymphoma cells and treated similarly with NPr-4-*S*-CAP. Cytotoxic activity of spleen effector cells against target B16F1 or RMA cells was determined by standard ^{51}Cr release assay.

2.7. Tetramer assay

Spleens and regional lymph nodes were removed on day 40 after primary melanoma resection. Lymphocytes prepared from regional lymph nodes were incubated at 37 °C for 30 min in the staining buffer (PBS with 0.1% BSA and 0.1% sodium azide) containing 10 μl of APC-labeled TYRP-2-specific tetramer (Medical & Biological Laboratories Co. Ltd., MBL, Nagoya, Japan). Cells were washed once, then incubated at 4 °C in the staining buffer containing 3 μg of anti-CD8a mAb conjugated to FITC (Becton,

Dickinson and Company (BD), NJ, USA). Lymphocytes prepared from spleens were stimulated with TYRP-2 peptide (2 mg/ml) for five days, then stained with APC-labeled TYRP-2-specific tetramer and FITC-labeled CD8a mAb. Samples were analyzed by FACS vantage using Cell QUEST software (BD). Lymphocytes were gated on $CD8^+$ cells. More than 10^5 events were acquired for each sample.

2.8. Cell proliferation assay

For assessment of the growth-inhibitory activities of NPr-4-*S*-CAP and NPr-2-*S*-CAP, NIH3T3, B16F1, 70W and M1 cells were dispensed at a density of 1.0×10^5 in 6-cm dishes and cultured for 24 h. Selected concentrations of NPr-4-*S*-CAP (0.5, 1.0, 2.0, and 3.0 mM), NPr-2-*S*-CAP (0.5, 1.0, 2.0, and 3.0 mM) or propylene glycol (120 μl) were added. After cells were cultured for 1 h, they were washed and refed with fresh DMEM and cultured for 24 h. The numbers of living cells that were not stained by trypan blue were counted and the average of 6 dishes was determined.

2.9. Flow cytometric analysis

B16F1, NIH3T3, RMA and TXM18 cells were cultured in the NPr-4-*S*-CAP-containing medium (1 mM) or propylene glycol for 1 h, they were washed in PBS and cultured for 24 h. For the positive control of apoptosis, TNF-related apoptosis-inducing ligand (TRAIL)/Apo2L (Wako, 2.0 μg/ml) was added and the cells were cultured for 24 h. Next, adherent and floating cells were collected together, washed in PBS, dehydrated in 70% cold ethanol and stored on ice for 2 h. They were then rehydrated in cold PBS and incubated in the presence of RNaseA (100 μg/ml) (Invitrogen) at 37 °C for 30 min. After incubation, the cells were rinsed twice in cold PBS and suspended in 2.0 ml of PBS containing 10 μg/ml propidium iodide (Wako) at 4 °C for 2 h. Sub G1, G1, S, and G2/M populations were quantified with a FACS Calibur flow cytometer (BD) using the Cell QUEST program.

2.10. Caspase enzyme assay

For this assay, 1.5×10^4 B16F1, NIH3T3, RMA and TXM18 cells were seeded in 96-well plates. After 24 h, the medium was replaced by one containing NPr-4-*S*-CAP or propylene glycol at the indicated concentrations followed by incubation for 1 h at 37 °C and washing with PBS. For positive control, cells were cultured in the presence of TRAIL/Apo2L and cultured for 24 h. After medium containing Caspase-Glo3/7 Assay kit solution (100 μl, Promega, Madison, WI) was added and the cells were cultured for 2 h, activity of caspase 3/7 was measured using a Wallac 1420 ARVO series multilabel reader (Perkin Elmer, MA, USA).

2.11. TUNEL assay

In order to assess the apoptosis in NPr-4-*S*-CAP mediated melanoma tumors, TUNEL assay was performed with an apoptosis detection kit (Takara Bio, Shiga, Japan). Tumors in group III and control groups processed according to Protocols 1 and 3 were harvested on day 22 as described above and fixed in formalin (4%, w/v) overnight. Samples were then dehydrated and embedded with paraffin. The staining was operated according to the manufacturer's instructions.

2.12. Fluorescence microscopy

Using a confocal fluorescence microscope (Radiance 2000MP, BIO-RAD, CA, USA), we studied the morphologic features of cell death induced by NPr-4-*S*-CAP. For this, 1.5×10^4 B16F1 and NIH3T3 cells were separately seeded on round glass coverslips that were coated with Atelo Cell IPC-30 (Koken Co. Ltd., Tokyo, Japan) and put into 12-well plates. They were cultured for 24 h with 5% FBS at 37 °C in a 5% CO_2 atmosphere. Cells were stained with 5 μM 5-(and-6)-chloromethyl-2′,7′-dichlorodihydro-fluorescein diacetate, acetyl ester (CM-H_2DCFDA, Invitrogen) for 30 min. They were then cultured in the medium containing NPr-4-*S*-CAP (1.0 mM) or propylene glycol (40 μl) for 1 h. After being cultured for 24 h, they were stained with a Rab pAb to Active Caspase 3 (Abcam, Cambridge, MA, USA), stained with Hoechst 33342 (10 μl per dish, Wako, Japan) and analyzed under a confocal microscope. The difference between apoptosis and necrosis was determined according to a previous report [15]; cells with nuclei showing aggregation and deformation were considered to be apoptotic and those with round nuclei to be necrotic.

2.13. Detection and analysis of intracellular ROS

After non-pigmented melanoma TXM18 and SK-mel-24 cell lines and pigmented melanoma B16F1, 70W, M-1 and G361 cells were cultured in medium containing 5 μM CM-H_2DCFDA (DCF, Invitrogen) for 30 min at 37 °C, they were washed with PBS, refed with medium containing NPr-2-*S*-CAP (1, 3, 6 mM) or NPr-4-*S*-CAP (0.5, 1, 2, 3, or 6 mM). After they were cultured for 1 h, they were washed in PBS and cultured for 24 h. For the positive control with exposure to ROS, the cells were cultured with H_2O_2 (0.5, 1, 2, 3 mM) for 24 h. Next, adherent and floating cells were collected together and processed for flow cytometry to quantify the M2 fraction using the Cell QUEST program (BD).

2.14. Statistical analyses

The data were analyzed by one- or two-way analysis of variance (ANOVA) and then differences in experimental results for tumor growth were assessed by Sheffe's test to compare all the experimental groups, or Dunnett's test for the experimental groups vs. the control group. For multiple comparisons the data were assessed by the log-rank test with Bonferroni correction. Differences in survival rates were analyzed by the Kaplan–Meier method. The level of significance was $P < 0.05$ (two-tailed). All statistical analyses were performed using StatView J-5.0 (SAS Institute Inc., Cary, NC, USA).

3. Results

3.1. NPr-4-S-CAP induces apoptotic cell death of B16F1 cells

B16F1, 70W and M-1 melanoma and NIH3T3 fibroblast cells were separately cultured in media containing different concentrations of NPr-4-*S*-CAP (0–3.0 mM) and NPr-2-*S*-CAP (0–3.0 mM). After a 24 h-incubation period, the anti-proliferative effect was assessed by cell-counting assay. Fig. 1 shows the effects of different concentrations of NPr-4-*S*-CAP and NPr-2-*S*-CAP on melanoma and NIH3T3 cells. The results indicated that NPr-4-*S*-CAP had a dose-dependent antiproliferative effect on B16F1, 70W and M-1 cells ($P < 0.05$, 51.6% of the relative cell number at the concentration of 3.0 mM in B16F1 cells) but not on NIH3T3 cells (83.7% at 3.0 mM). Conversely, NPr-2-*S*-CAP, an inactive form of CAP, did not have antiproliferative effects on B16F1 or NIH3T3.

To examine the mechanism of the cell death induced by NPr-4-*S*-CAP, these cells were subjected to flow cytometric analysis, caspase 3 assay and TUNEL staining. The sub-G1 fraction was increased in the NPr-4-*S*-CAP-treated B16F1 cells, comparable to TRAIL-exposed B16F1, but not in the NPr-4-*S*-CAP-treated non-melanoma cells (NIH3T3, RMA) or non-pigmented melanoma cells (TXM18) (Fig. 2A). The luminescent assay detected caspase 3/7 activity in the NPr-4-*S*-CAP-treated B16F1 cells remarkably

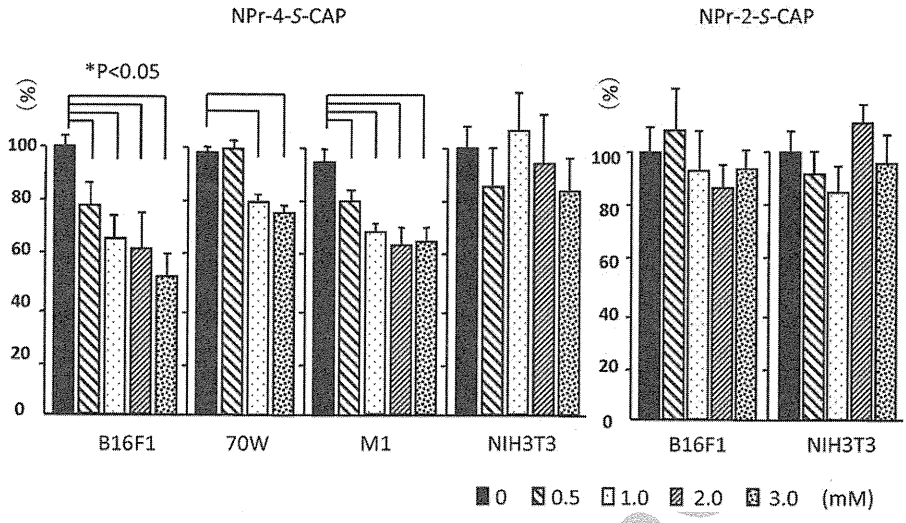

Fig. 1. NPr-4-*S*-CAP, but not NPr-2-*S*-CAP, suppresses growth of melanoma cells. The number of cells cultured in the medium containing NPr-4-*S*-CAP or NPr-2-*S*-CAP was counted as described in Section 2. All data are presented as mean ± standard deviation. Growth of B16F1, 70W and M-1 melanoma, but not NIH3T3 fibroblast cells, was suppressed by NPr-4-*S*-CAP ($P < .05$, Dunnett's test).

increased (35.8-fold) compared to that in the non-treated cells (Fig. 2B). NIH3T3, RMA and TXM18 cells treated with TRAIL showed 10.6, 7.1 and 5.8-fold increases of caspase 3/7 activation compared to the control, respectively, whereas those with NPr-4-*S*-CAP showed increases of 4.1, 1.4 and 1.8-fold, respectively (Fig. 2B). As shown in Fig. 2C, the number of TUNEL-positive cells was significantly increased only in the B16F1 tumor treated with NPr-4-*S*-CAP. This increase was not observed in the B16F1 tumor without NPr-4-*S*-CAP or in RMA tumors with or without NPr-4-*S*-CAP. These findings suggested that NPr-4-*S*-CAP induces apoptotic cell death selectively in pigmented melanoma cells.

3.2. NPr-4-S-CAP produces ROS

Melanoma cells produce ROS in the process of melanogenesis, possibly resulting in their degradation with disruption of cell

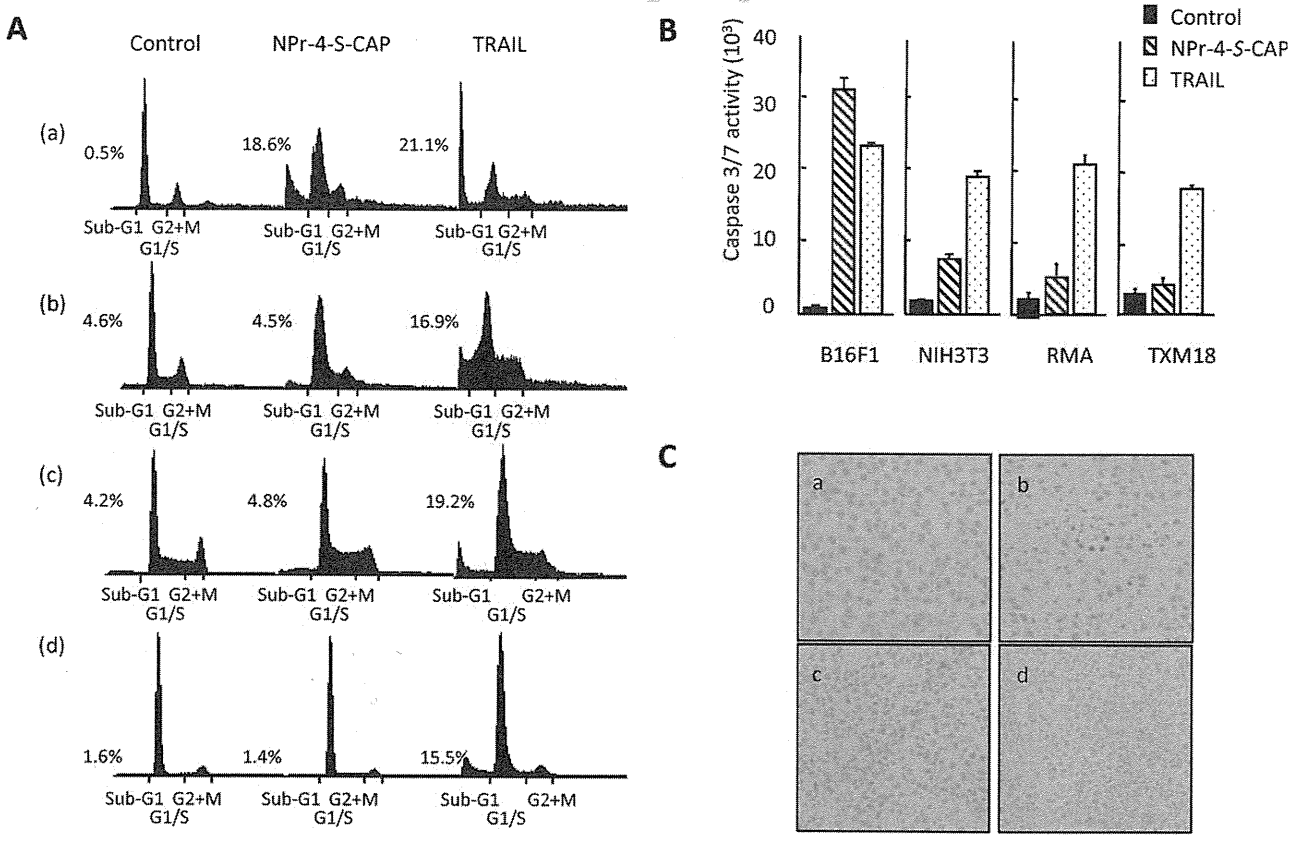

Fig. 2. NPr-4-*S*-CAP mediated apoptotic cell death of B16F1 melanoma cells. (A) Flow cytometric analysis of cellular DNA detected an increased sub-G1 fraction in NPr-4-*S*-CAP-treated B16F1 (a), but not NIH3T3 (b), RMA (c) or TXM18 (d). (B) Assay of caspase 3/7 in cells treated with NPr-4-*S*-CAP or TRAIL. Cells were cultured in the presence of NPr-4-*S*-CAP, TRAIL, or propylene glycol in 96-well plates and then processed for measurement of caspases 3 and 7 using a Caspase-Glo3/7 Assay kit. (C) Apoptosis of B16F1 tumors induced by NPr-4-*S*-CAP was assessed by the TUNEL method. Samples were obtained from (a) B16F1 tumors injected with propylene glycol, (b) B16F1 tumors treated with NPr-4-*S*-CAP, (c) RMA tumors injected with propylene glycol and (d) RMA injecteds with NPr-4-*S*-CAP. TUNEL-positive nuclei appear dark brown (200×).

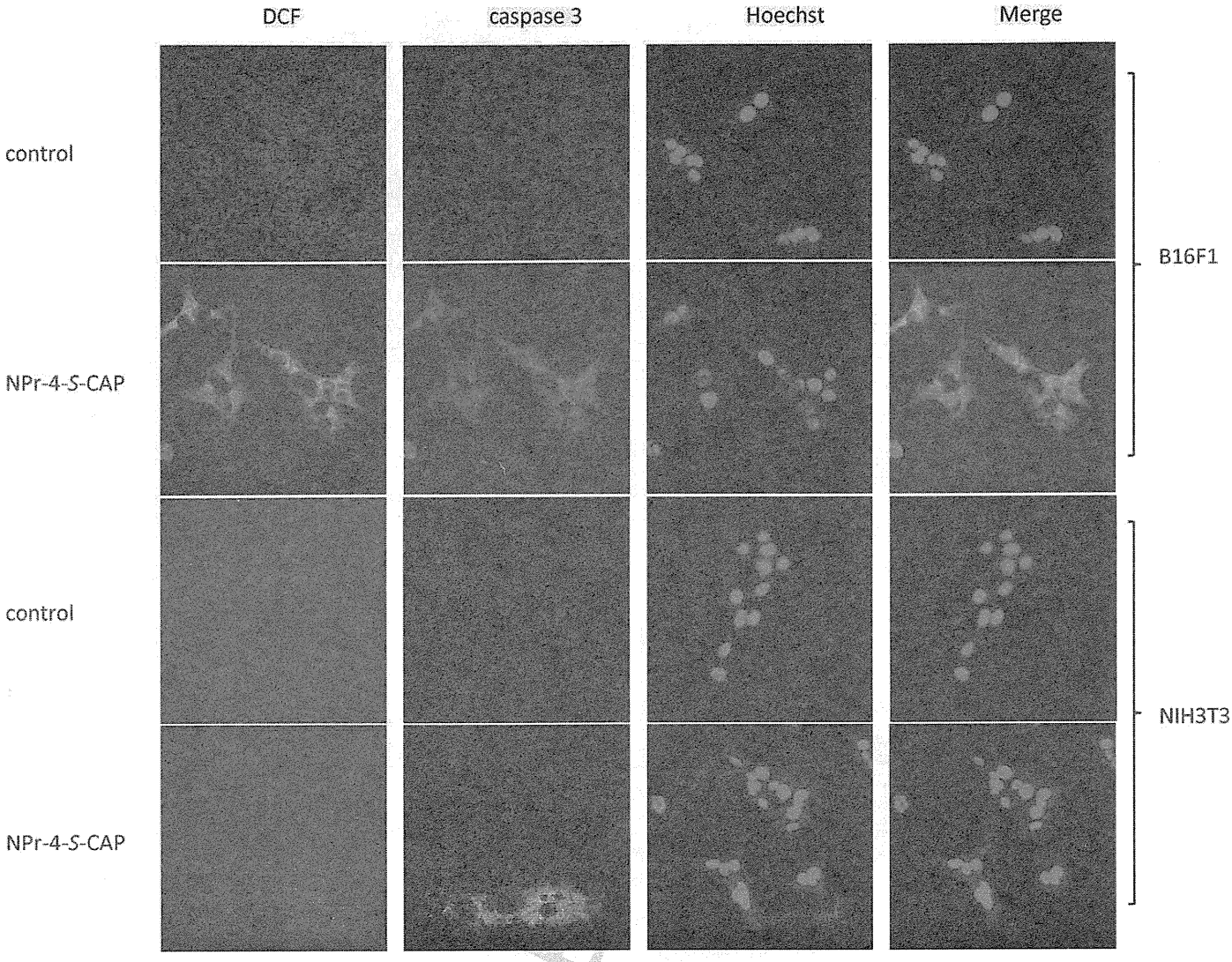

Fig. 3. Confocal microscopic observation of cells treated with NPr-4-*S*-CAP. B16F1 and NIH3T3 cells were stained with CM-H_2DCFDA for ROS production, a Rab pAb for activated caspase 3, and Hoechst 33342 for living nuclei.

membranes [16–18], but the molecular mechanism of NPr-4-*S*-CAP-mediated cell death has not yet been elucidated. To analyze the relations between NPr-4-*S*-CAP-mediated apoptosis and ROS production in B16F1 cells, we examined ROS generation and morphological changes using confocal fluorescent microscopy and flow cytometer. When B16F1 cells were cultured in the medium containing NPr-4-*S*-CAP, about half of their nuclei were aggregated and deformed, which was associated with an increase of ROS and caspase 3 in their cytoplasm (Fig. 3). NIH3T3 cells, however, did not show any of these changes (Fig. 3). When pigmented (B16F1, 70W, M-1 and G361) and non-pigmented (TXM18 and SK-mel-24) melanoma cells were treated with NPr-4-*S*-CAP, ROS production was selectively observed in the pigmented melanoma cell lines (Fig. 4). These findings suggested that NPr-4-*S*-CAP selectively produced ROS in pigmented melanoma cells such as B16F1 and that ROS played an important role in the NPr-4-*S*-CAP-associated apoptosis.

3.3. NPr-4-S-CAP suppresses growth of primary and secondary B16F1 tumors in mice

To examine whether NPr-4-*S*-CAP had an anti-melanoma effect, syngeneic mice bearing B16F1 tumors were given NPr-4-*S*-CAP by intratumoral injections and the volumes of tumors are measured as described in Section 2. First, we compared the direct effects of NPr-4-*S*-CAP and NPr-2-*S*-CAP on the transplanted B16F1 melanomas. Growth of tumors injected with NPr-4-*S*-CAP was remarkably suppressed ($P = .0247$ by a Sheffe test), but those treated with NPr-2-*S*-CAP, like control mice, were not affected (Fig. 5). The mice were divided into four different groups, a non-treated control group, and treated groups I, II and III. Tumors in group II (injected every other day for a total of five times) and group III (injected for five consecutive days), especially, showed significant reductions in their volumes compared to those of control mice by day 20 ($P = .0163$ and .0100, respectively, vs. control group, Fig. 6A). On the other hand, NPr-4-*S*-CAP did not affect the tumor volume of transplanted RMA T-cell lymphoma (Fig. 6B). These results suggested that NPr-4-*S*-CAP had a selective chemotherapeutic effect on B16F1 melanoma cells.

We then examined whether secondary B16F1 tumors transplanted on the opposite flank were suppressed after the treatment of primary tumors with NPr-4-*S*-CAP. In all the treated groups (I, II and III), tumor growth after rechallenge with secondary B16F1 melanomas was suppressed (Fig. 6C). The tumor volumes of groups II and III were significantly reduced compared to those of the control mice ($P = .0321$ and .0160, respectively, Fig. 6C). However,

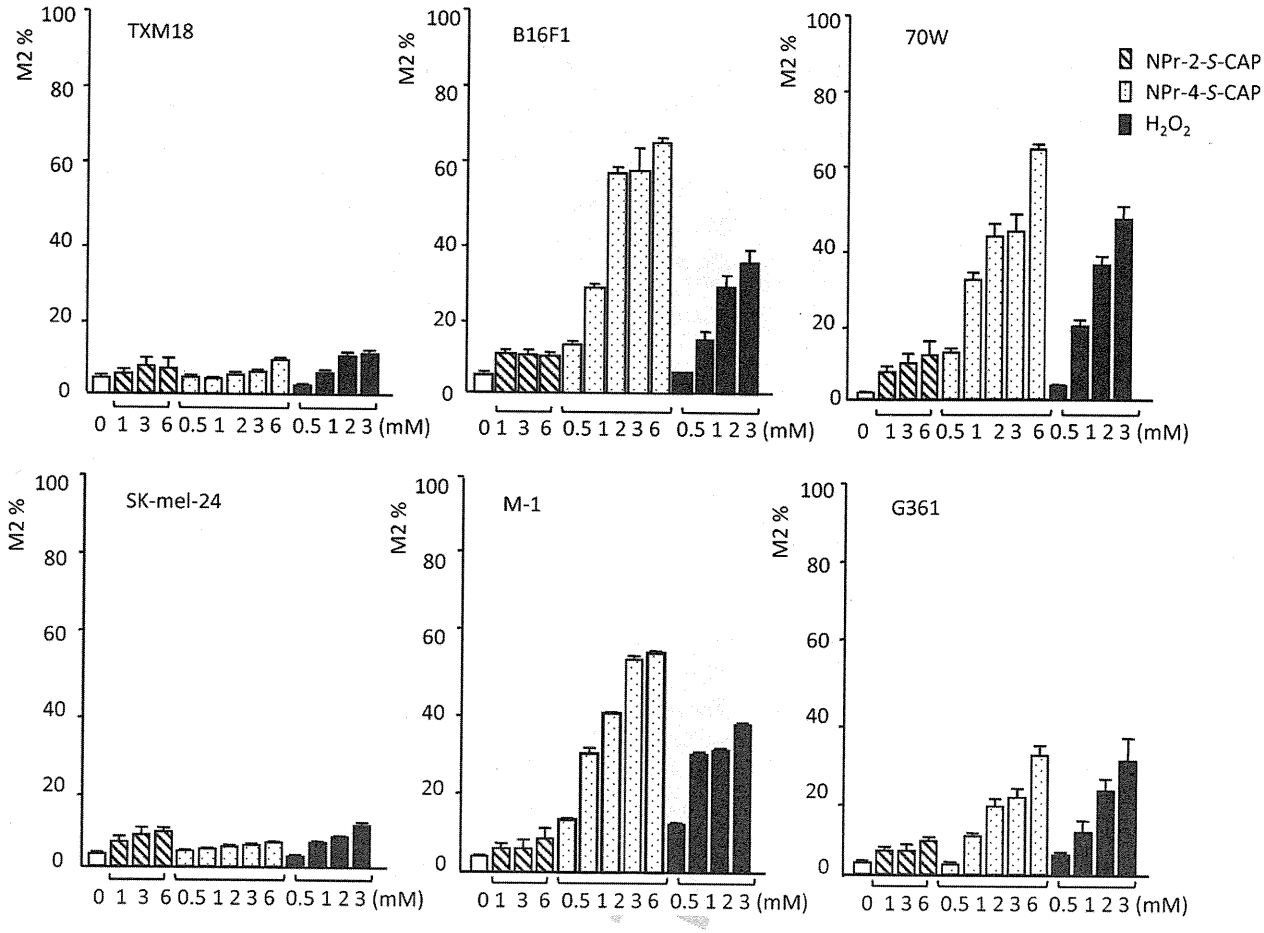

Fig. 4. Pigmented melanoma but not non-pigmented melanoma cells produce ROS in the presence of NPr-4-*S*-CAP. Cells were cultured in the presence of MDCF for 30 min, washed twice with PBS, refed with medium containing NPr-2-*S*-CAP or NPr-4-*S*-CAP and cultured for a further 1 h. They were then harvested and processed for FACScan analysis.

secondary RMA T-cell lymphoma tumors were not suppressed when they were transplanted after the primary B16F1 tumors were removed (Fig. 6D). The survival periods and survival rates of mice among the four groups were observed for as long as 120 days. Significant prolongations of survival were observed in groups I, II and III compared to the control group (P = .0177, .0024 and .0435, respectively, Fig. 7A).

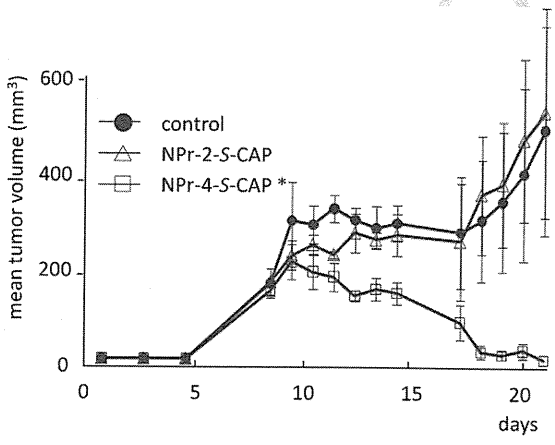

Fig. 5. NPr-4-*S*-CAP, but not NPr-2-*S*-CAP, suppresses growth of transplanted B16F1 tumors. The syngeneic mice bearing B16F1 tumors were given 24.4 μmol NPr-4-*S*-CAP or NPr-2-*S*-CAP in five consecutive intratumoral injections and the volumes of tumors were measured.

In the histopathological examination against primary and secondary transplanted B16F1 or RMA tumors, a dense inflammatory infiltrate including neutrophils, macrophages, plasma cells and lymphocytes was observed around NPr-4-*S*-CAP treated B16F1 tumors which were harvested on day 22 (Fig. 8E and F). Furthermore, we observed that numerous $CD8^+$ T cells were infiltrated within these tumors (Fig. 8H). By contrast, inflammatory cells were not detectable in the primary B16F1 tumors without treatment or RMA tumors with or without treatment (Fig. 8A and B, data not shown for RMA tumors). $CD4^+$ T cells were not infiltrated in either these tumors (Fig. 8C and G). In the secondary B16F1 tumors, the inflammatory cells were infiltrated around the residual tumor but the density of $CD4^+$ and $CD8^+$ T cells was not prominent as the treated primary tumors (data not shown).

3.4. $CD8^+$ T cells mediate suppression of rechallenge with B16F1 melanoma

Six weeks after the NPr-4-*S*-CAP injections, vitiligo (depigmented cutaneous lesions) or a change in hair color to white appeared in two of the six mice in group III in areas of the body distant from the injection points (Fig. 7B). This suggested that the vitiligo was not generated by a direct effect of NPr-4-*S*-CAP but by the induction of systemic tumor-specific T-cell immunity against melanocytes. To analyze the mechanism of the anti-melanocyte immunity induced by NPr-4-*S*-CAP, in vivo T cell depletion assay was performed. When B16F1 melanoma-bearing mice were injected with an anti-CD8 antibody i.p., tumor growth was not

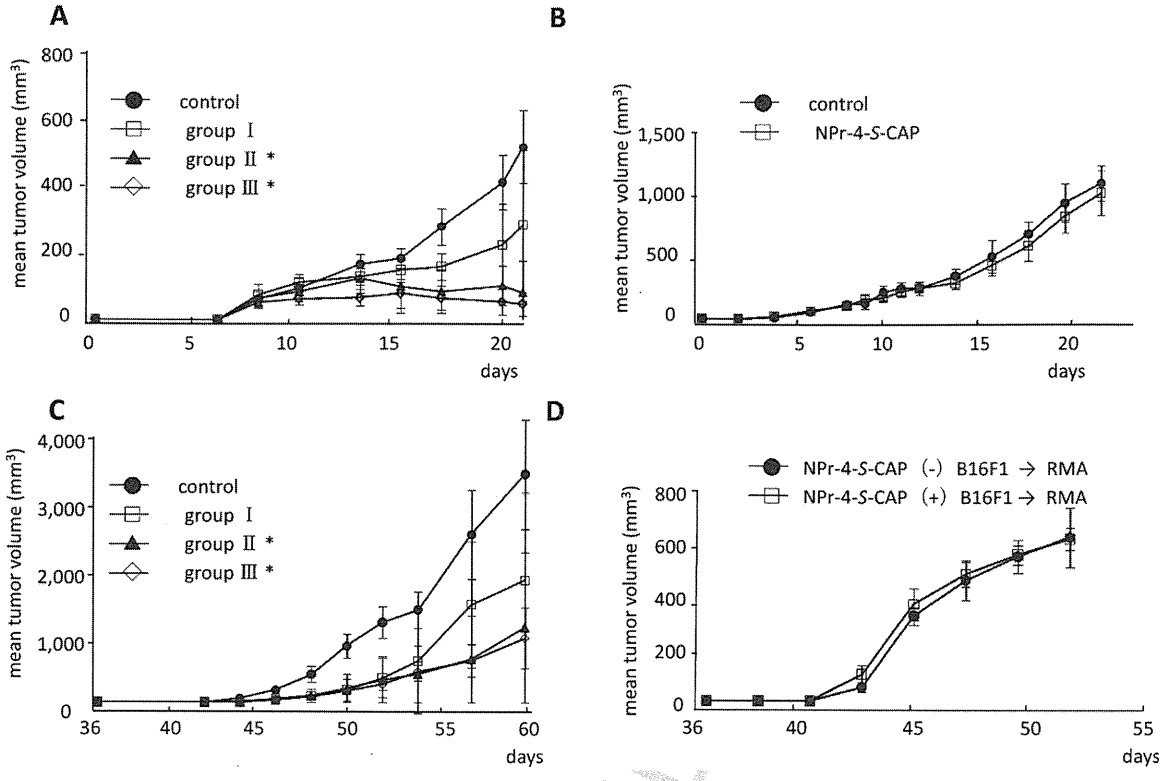

Fig. 6. NPr-4-*S*-CAP suppresses growth of primary and secondary rechallenge B16F1 melanomas. (A) Mice were transplanted with B16F1 cells and treated with NPr-4-*S*-CAP. Tumor volumes of treated groups I, II and III were suppressed. In particular, tumors in groups II and III showed significant reductions in their volumes ($P < .05$). (B) Transplanted RMA mouse T lymphomas were injected with NPr-4-*S*-CAP and tumor volumes were measured. (C) Tumor volumes of secondary B16F1 melanomas in mice belonging to groups I, II and III. Growth of rechallenge melanomas on the opposite flanks was markedly suppressed in the mice of groups II and III. (D) Growth of secondarily transplanted RMA lymphomas was not inhibited in mice after the primary B16F1 tumors were removed.

suppressed. However, the growth of tumors remained significantly suppressed (i.e., it was not further affected) after injection of an anti-CD4 antibody or Rat IgG i.p. ($P = .0167$ vs. rat IgG group, Fig. 9). This suggested that $CD8^+$ T cells participated in the NPr-4-*S*-CAP-mediated anti-B16F1 immunity.

To analyze whether tumor-specific immunity had been induced, CTL induction was examined by Cr-release assay and tetramer assay. Spleen cells were obtained from the cured mouse and mixed with B16F1 cells to detect their specific lyses. As shown in Fig. 10A, spleen cells showed cytotoxic activity to B16F1 cells but not to the non-melanoma RMA cells. However, spleen cells from the naïve or RMA-challenged mice did not show cytotoxic activity to either B16F1 or RMA cells. For the tetramer assay, splenocytes were prepared from a naïve mouse and from mice with B16F1 or RMA tumors after treatment with NPr-4-*S*-CAP, and stimulated in vitro with TYRP-2 peptide for five days.

Recovered splenocytes were stained with TYRP-2-specific tetramer, and proportions of peptide-specific $CD8^+$ T cells were

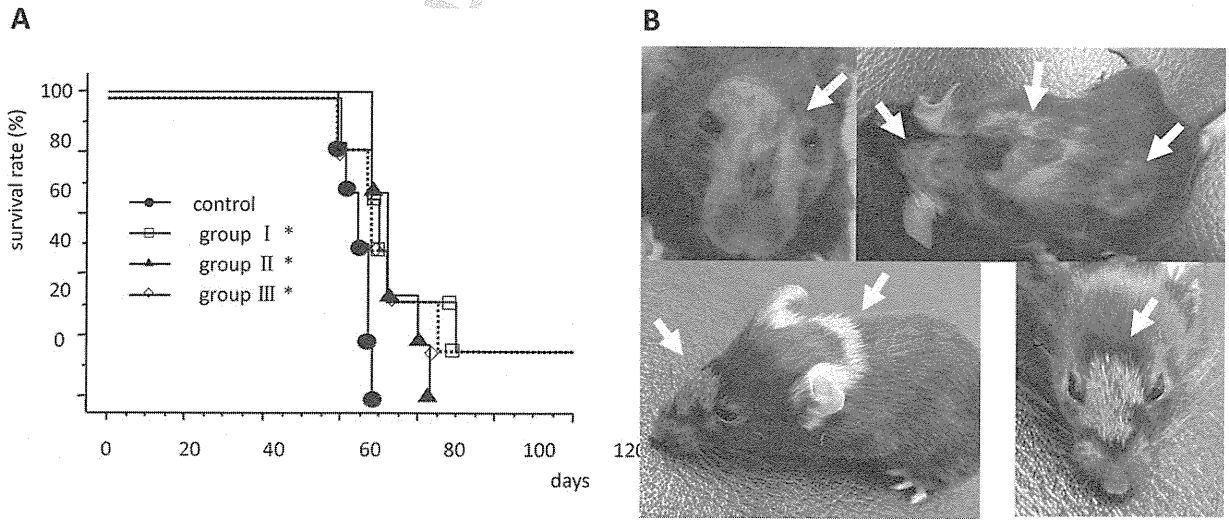

Fig. 7. (A) The survival periods and survival rates of tumor-bearing mice. Kaplan–Meier survival curves over a period of 120 days after the tumor transplantation showed that significant prolongations of survival were observed in groups I, II and III compared to the control mice ($P = .0177$, $P = .0024$ and $P = .0435$, respectively, vs. control). (B) Appearance of vitiligo on the treated mice. Six weeks after the NPr-4-*S*-CAP injection, vitiligo or white hair appeared at body sites distant from the injection point.

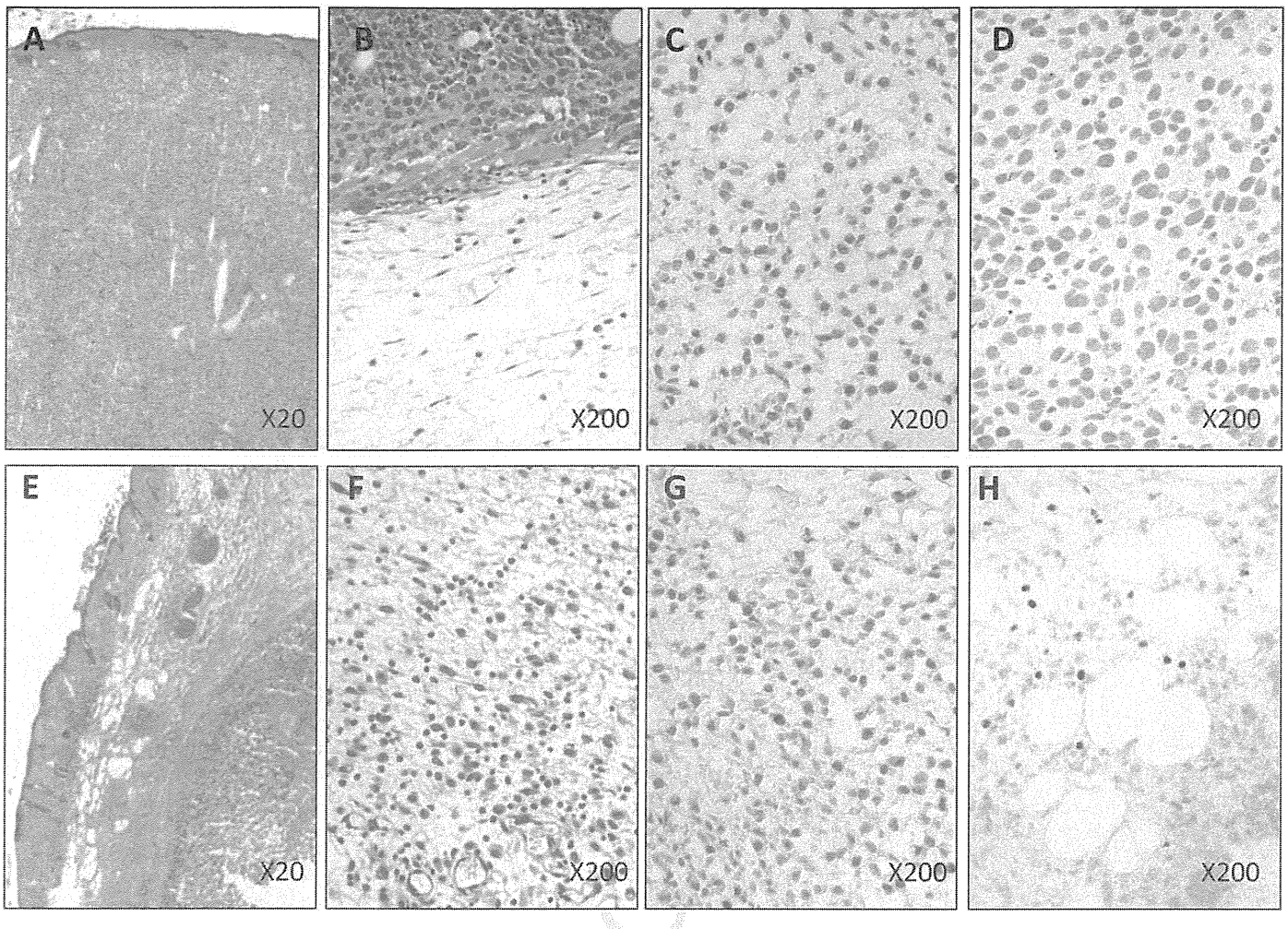

Fig. 8. Dense inflammatory cells and CD8$^+$ T cells were infiltrated in NPr-4-*S*-CAP treated B16F1 tumors. The B16F1 tumors were harvested on day 22 and histopathological features were analyzed by HE-staining (A, B, E, F) or an anti-mouse CD4 mAb (C, G) or CD8 mAb (D, H).

determined. As shown in Fig. 10B, 9.08% of the CD8$^+$ T cells in the B16F1-challenged mice treated with NPr-4-*S*-CAP were specific for the TYRP-2 peptide, compared with 2.66% or 2.96% in the naïve or RMA-challenged mice, respectively. In addition, lymphocytes isolated from the regional lymph node of RMA or B16F1 transplanted into mice treated with NPr-4-*S*-CAP, were also stained with TYRP-2-specific tetramer. As shown in Fig. 10B, 8.14% of the CD8$^+$ T cells in the B16F1-challenged mice treated with NPr-4-*S*-CAP were specific for the TYRP-2 peptide, compared with 5.43% or 4.89% in the naïve or RMA-challenged mice, respectively.

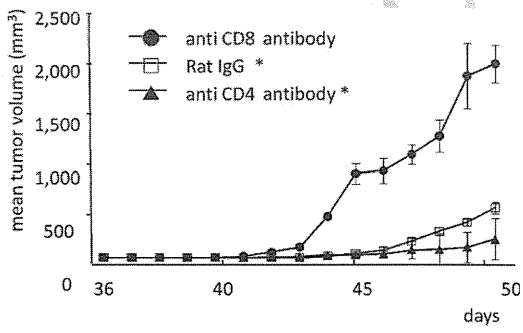

Fig. 9. Suppression of secondary tumors is inhibited by an anti-CD8 antibody. After the first challenge, the mice from group III were injected with 0.2 mg of anti-CD4, anti-CD8 or rat IgG i.p. on days 29 and 43, one week before and after the rechallenge by B16F1 transplantation, respectively.

The results from the two independent CTL assays were highly consistent, showing that the NPr-4-*S*-CAP treatment to B16F1 melanoma produced a functional CTL response.

4. Discussion

Although selective cytotoxicities and anti-melanoma effects of cysteaminyl phenol derivatives have been reported, the mechanisms of cell death induced by the compounds have not been elucidated. Here, we demonstrated that NPr-4-*S*-CAP induced apoptosis selectively in pigmented melanoma cells in association with ROS production and caspase 3 activation. In addition, this is the first report demonstrating that NPr-4-*S*-CAP can induce host T-cell immune responses associated with rejection of in vivo rechallenge with melanoma.

Tyrosinase inhibitors with simple skeletal structures similar to phenol such as hydroquinone, kojic acid, arbutin and deoxyarbutin have been used as skin whitening agents via topical application [19]. Administration of a melanin precursor such as 4-*S*-cysteaminylphenol to black mice resulted in depigmentation of hair follicles, possibly by the selective disintegration of melanocytes in the hair bulb [10,14,20–22]. NPr-4-*S*-CAP exerts strong cytotoxicity toward melanoma cells, in which melanin synthesis is highly elevated [8,9,11]. When phenolic amine compounds are oxidized by tyrosinase, melanin intermediates inhibit the activity of SH enzymes such as thymidylate synthase, alcohol dehydrogenase and DNA polymerase by covalent binding through their

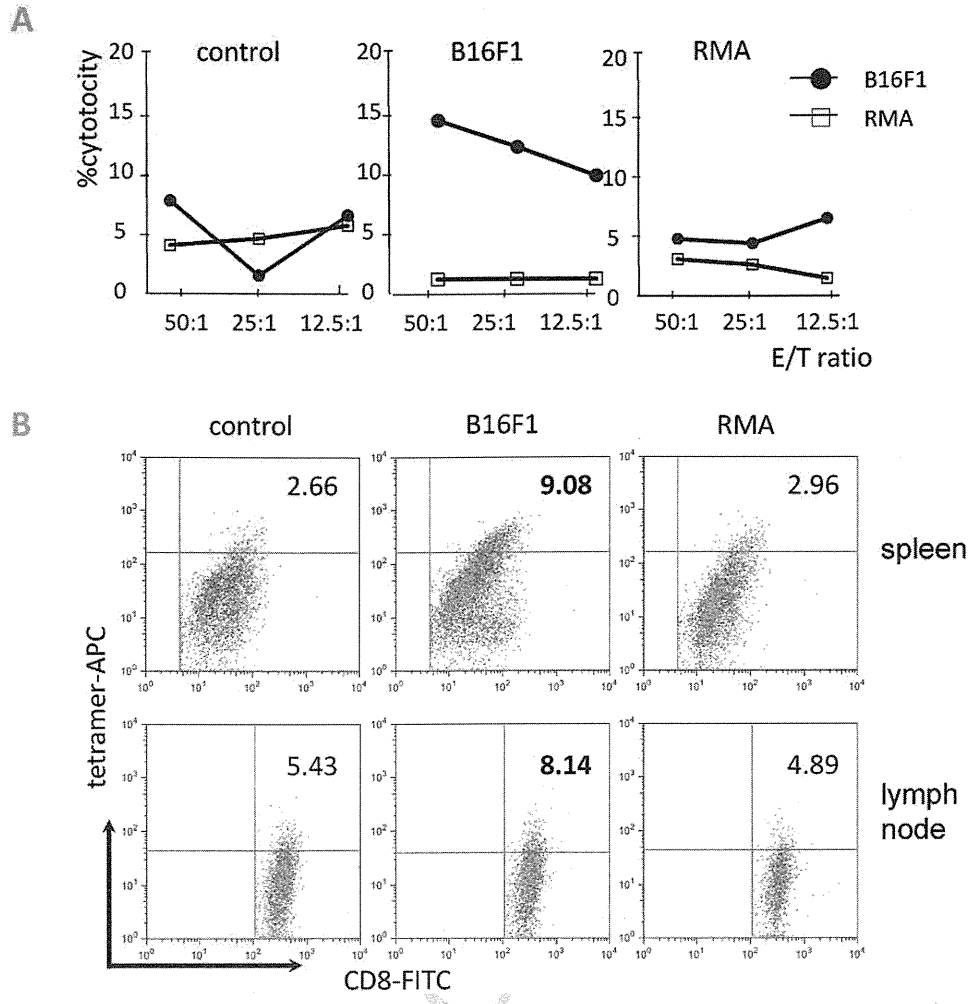

Fig. 10. Splenocytes and/or lymphocytes of tumor-bearing mice contain CTL activity against B16F1 cells detectable by ^{51}Cr assay (A) and tetramer assay (B). (A) After the first challenge, the spleen cells from naïve mice (control) and B16F1- or RMA-challenged mice treated with NPr-4-*S*-CAP were harvested from the mice and cytotoxic activity of effector cells against target cells (B16F1 and RMA) was determined by standard ^{51}Cr assay. T, tumor B16F1 cells; E, effector spleen cells. (B) Splenocytes and lymphocytes from naïve mice (control), RMA- or B16F1-challenged mice treated with NPr-4-*S*-CAP were stained with APC-labeled TRP-2-specific tetramer together with FITC-labeled anti-CD8 mAb. The numbers shown represent the percentage of tetramer$^+$ cells within CD8$^+$ T lymphocytes.

cysteine residues, resulting in melanoma-specific cytotoxicity [23–25].

In the present study, NPr-4-*S*-CAP suppressed growth of cultured melanoma cells and induced apoptotic cell death accompanied by ROS generation. Since pigmented melanoma cells (B16F1, 70W, G361 and M-1), but not non-pigmented ones (TXM18 and SK-mel-24), produced significant amounts of ROS (Fig. 4) in the presence of NPr-4-*S*-CAP, it was suggested that melanin biosynthesis was essential for NPr-4-*S*-CAP to produce ROS. It has been reported that ROS-mediated apoptosis is initiated via two pathways, the death receptor (Fas ligand–Fas receptor) and the mitochondria-mediated pathway in which the Trx/ASK1 complex acts as a redox switch to release cytochrome C [26,27]. Intracellular ROS mediate apoptotic cell death, which elicits a strong host inflammation reaction and subsequent induction of host immune responses [28]. Transcription factor NF-E2-related factor 2 (Nrf2) is activated by ROS to induce cellular genes such as glutathione-*S*-transferase, heme oxygenase and glucose-6-phosphodehydrogenase to protect cells from oxidative stress [29,30]. It is possible that Nrf2-1 and/or its related genes could not be induced to a level sufficient for the protection of melanoma cells from oxidative stress.

In the mouse model of thermotherapy for B16 melanoma, it has been suggested that HSPs, especially HSP70 and HSP72, are involved in tumor-specific CTL responses [31,32]. We suggested in a previous report that the CTL response against B16-OVA melanoma induced by hyperthermia using NPrCAP/M was associated with the release of the HSP72-peptide complex from degraded tumor cells [33]. In the present study, we therefore examined whether HSPs were induced in and released from melanoma cells after injection of NPr-4-*S*-CAP; however, Western blot analysis did not detect an increase of HSP72 or HSP90 in the NPr-4-*S*-CAP-treated B16F1 cells (data not shown). Thus, although intracellular HSPs may play a role in the induction of NPr-4-*S*-CAP-mediated antitumor immunity, the induction of HSPs is not a prerequisite for the NPr-4-*S*-CAP-mediated tumor-specific immune response.

Results of the in vivo T cell depletion assay using anti-CD8 antibodies, Cr-releasing assay and tetramer assay using B16F1 and spleen cells from NPr-4-*S*-CAP-treated and cured mice suggested that suppression of the primary tumor by NPr-4-*S*-CAP was able to induce CD8$^+$ T cell immunity against component of B16F1 melanoma. Melanoma tumor antigens recognized by T lymphocytes are derived from melanocyte differentiation antigens (tyrosinase, TYRP-1, TYRP-2 and gp100), tumor testis antigens (NY-ESO-1, MAGE1 and MEGE3) and mutated cellular gene products (β-catenin and p53). In mouse B16 melanoma model, TYRP-2 is reported to be a strong melanoma rejection antigen since

tolerance to TYRP-2 can be broken by TYRP-2 vaccination and TYRP-2-specific CTCLs mediate anti-tumor immunity [34–36]. Although it is not clear which B16F1 tumor antigens were presented on the dendritic cells for induction of $CD8^+$ T cells, in comparison with the naïve or RMA-transplanted mice, increased frequency of $CD8^+$ T cells specific for the TYRP-2 peptide were detected in B16F1-challenged mice treated with NPr-4-*S*-CAP. This suggested that TYRP-2 was a part, but not all, of a tumor antigen associated with rejection of B16 melanoma.

Recently, Westerhof et al. proposed the haptenation theory in which increased intracellular H_2O_2 could trigger the increased turnover of elevated levels of surrogate substrates of tyrosinase, resulting in melanocyte-specific T-cell responses [37,38]. According to this hypothesis, tyrosinase would be recognized as a melanoma-specific tumor antigen in relation to the systemic immune responses. This line of study may contribute to the clinical application of NPr-4-*S*-CAP for therapy targeting malignant melanoma.

Acknowledgments

This work was supported by Health and Labor Sciences Research Grants-in-Aid (H17-nano-004 and H21-nano-006) for Research on Advanced Medical Technology from the Ministry of Health, Labor and Welfare of Japan.

References

[1] Ishihara K, Saida T, Yamazaki N. Prognosis and Statistical Investigation Committee of the Japanese Skin Cancer Society. Statistical profiles of malignant melanoma and other skin cancers in Japan: 2007 update. Int J Clin Oncol 2008;13:33–41.
[2] Balch CM, Gershenwald JE, Soong SJ, Thompson JF, Atkins MB, Byrd DR, et al. Final version of 2009 AJCC melanoma staging and classification. J Clin Oncol 2009;27:6199–206.
[3] Rad HH, Yamashita T, Jin HY, Hirosaki K, Wakamatsu K, Ito S, et al. Tyrosinase-related proteins suppress tyrosinase-mediated cell death of melanocytes and melanoma cells. Exp Cell Res 2004;298:317–28.
[4] Jimbow K, Miura S, Ito Y, Kasuga T, Ito S. Utilization of melanin precursors for experimental chemotherapy of malignant melanoma. Jpn J Cancer Chemother 1984;11:2125–32.
[5] Ito S, Kato T, Ishikawa K, Kasuga T, Jimbow K. Mechanism of selective toxicity of 4-S-cysteinylphenol and 4-S-cysteaminylphenol to melanocytes. Biochem Pharmacol 1987;36:2007–11.
[6] Pankovich JM, Jimbow K, Ito S. 4-S-cysteaminylphenol and its analogues as substrates or tyrosinase and monoamine oxide. Pigment Cell Res 1990;3: 146–9.
[7] Miura T, Jimbow K, Ito S. The in vivo antimelanoma effect of 4-S-cysteaminylphenol and its N-acetyl derivative. Int J Cancer 1990;46:931–4.
[8] Alena F, Iwashita T, Gili A, Jimbow K. Selective in vivo accumulation of N-acetyl-4-cysteaminylphenol in B16F10 murine melanoma effect by combination of buthionine sulfoximine. Cancer Res 1994;54:2661–6.
[9] Tandon M, Thomas PD, Shokravi M, Singh S, Samra S, Chang D, et al. Synthesis and antitumor effect of the melanogenesis-based antimelanoma agent N-propionyl-4-S-cysteaminylphenol. Biochem Pharmacol 1998;55:2023–9.
[10] Minamitsuji Y, Toyofuku K, Sugiyama S, Yamada K, Jimbow K. Sulfur containing tyrosine analogs can cause selective melanocytotoxicity involving tyrosinase-mediated apoptosis. J Invest Dermatol Symp Proc 1999;4:130–6.
[11] Thomas PD, Kishi H, Cao H, Ota M, Yamashita T, Singh S, et al. Selective incorporation and specific cytocidal effect as the cellular basis for the antimelanoma action of sulphur containing tyrosine analogs. J Invest Dermatol 1999;113:928–34.
[12] Sato M, Yamashita T, Okura M, Osai Y, Sato A, Takada T, et al. N-propionyl-cysteaminylphenol–magnetite conjugate (NPrCAP/M) is a nanoparticle for the targeted growth suppression of melanoma cells. J Invest Dermatol 2009; 129:2233–41.
[13] Eikawa S, Ohue Y, Kitaoka K, Aji T, Uenaka A, Oka M, et al. Enrichment of Foxp3+ CD4 regulatory T cells in migrated T cells to IL-6- and IL-8-expressing tumors through predominant induction of CXCR1 by IL-6. J Immunol 2010;185:6734–40.
[14] Miura S, Ueda T, Jimbow K, Ito S, Fujita K. Synthesis of cysteinylphenol, cysteaminylphenol, and related compounds, and in vivo evaluation of anti-melanoma effect. Arch Dermatol Res 1987;279:219–25.
[15] Shimizu S, Eguchi Y, Kamiike W, Itoh Y, Hasegawa J, Yamabe K, et al. Induction of apoptosis as well as necrosis by hypoxia and predominant prevention of apoptosis by Bcl-2 and Bcl-X_L. Cancer Res 1996;56:2161–6.
[16] Rotman A, Daly JW, Creveling CR. Oxygen-dependent reaction of 6-hydroxydopamine,5,6-dihydroxytryptamine and related compounds with proteins in vivo: a model for cytotoxicity. Mol Pharmacol 1976;12:887–99.
[17] Ito S, Inoue S, Fujita K. The mechanism of toxicity of 5-S-cysteinyldopa to tumour cells. Hydrogen peroxide as a mediator of cytotoxicity. Biochem Pharmacol 1983;32:2079–81.
[18] Yamada K, Jimbow K, Engelhardt R, Ito S. Selective cytotoxicity of a phenolic melanin precursor, 4-S-cysteaminylphenol, on in vitro melanoma cells. Biochem Pharmacol 1989;38:2217–21.
[19] Solano F, Briganti S, Picardo M, Ghanem G. Hypopigmenting agents: an updated review on biological, chemical and clinical aspects. Pigment Cell Res 2006;19:550–71.
[20] Ito Y, Jimbow K, Ito S. Depigmentation of black guinea pig skin by topical application of cysteaminylphenol, cysteinylphenol, and related compounds. J Invest Dermatol 1987;88:77–82.
[21] Ito Y, Jimbow K. Selective cytotoxicity of 4-S-cysteaminylphenol on follicular melanocytes of the black mouse: rational basis for its application to melanoma chemotherapy. Cancer Res 1987;47:3278–86.
[22] Jimbow K, Iwashina T, Alena F, Yamada K, Pankovich J, Umemura T. Exploitation of pigment biosynthesis pathway as a selective chemotherapeutic approach for malignant melanoma. J Invest Dermatol 1993;100:S231–8.
[23] Wick MM. Levodopa and dopamine analogs as DNA polymerase inhibition and antitumor agents in human melanoma. Cancer Res 1980;40:1414–8.
[24] Yamada I, Seki S, Ito S, Matsubara O, Kasuga T. The killing effect of 4-S-cysteaminylphenol, a newly synthesized melanin precursor, on B16 melanoma cell lines. Br J Cancer 1991;63:187–90.
[25] Hasegawa K, Ito S, Inoue S, Wakamatsu K, Ozeki H, Ishiguro I. Dihydroxy-1,4-benzothiazine-6,7-dione, the ultimate toxic metabolite of 4-S-cysteaminylphenol and 4-S-cysteaminylcatechol. Biochem Pharmacol 1997;53:1435–44.
[26] Denning TL, Takaishi H, Crowe SE, Boldogh I, Jevnikar A, Ernst PB. Oxidative stress induces the expression of Fas and Fas ligand and apoptosis in murine intestinal epithelial cells. Free Radic Biol Med 2002;33:1641–50.
[27] Circu ML, Aw TY. Reactive oxygen species, cellular redox systems, and apoptosis. Free Radic Biol Med 2010;48:749–62.
[28] Shellman YG, Howe WR, Miller LA, Goldstein NB, Pacheco TR, Mahajan RL, et al. Hyperthermia induces endoplasmic reticulum-mediated apoptosis in melanoma and non-melanoma skin cancer cells. J Invest Dermatol 2008; 128:949–56.
[29] Itoh K, Mochizuki M, Ishii Y, Ishii t, Shibata T, Kawamoto Y, et al. Transcription factor Nrf2 regulates inflammation by mediating the effect of 15-deoxy-$\Delta^{12,14}$-prostaglandin J_2. Mol Cell Biol 2004;24:36–45.
[30] Jian Z, Li K, Liu L, Zhang Y, Zhou Z, Li C, et al. Heme oxygenase-1 protects human melanocytes from H_2O_2-induced oxidative stress via the Nrf2-ARE pathway. J Invest Dermatol 2011;131:1420–7.
[31] Ito A, Tanaka K, Kondo K, Shinkai M, Honda H, Matsumoto K, et al. Tumor regression by combined immunotherapy and hyperthermia using magnetic nanoparticles in an experimental subcutaneous murine melanoma. Cancer Sci 2003;94:308–13.
[32] Suzuki M, Shinkai M, Honda H, Kobayashi T. Anticancer effect and immune induction by hyperthermia of malignant melanoma using magnetite cationic liposomes. Melanoma Res 2003;13:129–35.
[33] Sato A, Tamura Y, Sato N, Yamashita T, Takada T, Sato M, et al. Melanoma-targeted chemo-thermo-immuno (CTI)-therapy using N-propionyl-4-S-cysteaminylphenol-magnetite nanoparticles elicits CTL response via heat shock protein–peptide complex release. Cancer Sci 2010;101:1939–46.
[34] Bronte V, Apolloni E, Ronca R, Zamboni P, Overwijk WW, Surman DR, et al. Genetic vaccination with "self" tyrosinase-related protein 2 causes melanoma eradication but not vitiligo. Cancer Res 2000;60:253–8.
[35] Mendiratta SK, Thai G, Eslahi NK, Thull NM, Matar M, Bronte V, et al. Therapeutic tumor immunity induced by poluimmunization with melanoma antigens gp100 and TRP-2. Cancer Res 2001;61:859–63.
[36] Ji Q, Gondek D, Hurwitz AA. Provision of granulocyte–macrophage colony-stimulating factor converts an autoimmune response to a self-antigen into an antitumor response. J Immunol 2005;175:1456–63.
[37] Westerhof W, d'Ischia M. Vitiligo puzzle: the pieces fall in place. Pigment Cell Res 2007;20:345–59.
[38] Westerhof W, Manini P, Napolitano A, d'Ischia M. The haptenation theory of vitiligo and melanoma rejection: a close-up. Exp Dermatol 2011;20:92–6.

Journal of Biomaterials and Nanobiotechnology, 2012, 3, ***-***
Published Online April 2012 (http://www.SciRP.org/journal/jbnb)

Scientific Research

Conjugation of Magnetite Nanoparticles with Melanogenesis Substrate, NPrCAP Provides Melanoma Targeted, *in Situ* Peptide Vaccine Immunotherapy through HSP Production by Chemo-Thermotherapy

Kowichi Jimbow[1,3], Yasuaki Tamura[2], Akihiro Yoneta[3], Takafumi Kamiya[3], Ichiro Ono[3], Toshiharu Yamashita[3], Akira Ito[4], Hiroyuki Honda[5], Kazumasa Wakamatsu[6], Shosuke Ito[6], Satoshi Nohara[7], Eiichi Nakayama[8] and Takeshi Kobayashi[9]

[1]Institute of Dermatology & Cutaneous Sciences, Sapporo, Japan; [2]Department of Pathology 1, Sapporo Medical University School of Medicine, Sapporo, Japan; [3]Department of Dermatology, Sapporo Medical University School of Medicine, Sapporo, Japan; [4]Department of Chemical Engineering, Faculty of Engineering, Kyushu University, Fukuoka, Japan; [5]Department of Biotechnology, School of Engineering, Nagoya University, Nagoya, Japan; [6]Department of Chemistry, Fujita Health University School of Health Sciences, Toyoake, Japan; [7]Meito Sangyo Co., Nagoya, Japan; [8]Faculty of Health and Welfare, Kawasaki University of Medical Welfare, Kurashiki, Japan; [9]Department of Biological Chemistry, College of Bioscience and Biotechnology, Chubu University, Kasugai, Japan.
Email: jimbow@sapmed.ac.jp

Received ********** 2012

ABSTRACT

In order to develop melanoma-targeted *in situ* peptide vaccine immunotherapy, magnetite nanoparticles were conjugated with a melanogenesis substrate, N-propionyl cysteaminylphenol (NPrCAP). Magnetite nanoparticles introduced thermotherapy which caused non-apoptotic cell death and generation of heat shock protein (HSP) upon exposure to alternating magnetic field (AMF). NPrCAP was expected to develop a melanoma-targeted therapeutic drug because of its selective incorporation into melanoma cells and production of highly reactive free radicals, that result in not only oxidative stress but also apoptotic cell death by reacting with tyrosinase.

Keywords: Melanogenesis; Chemo-Thermo-Immunotherapy; Nanomedicine; Melanoma; Magnetite Nanoparticles

1. Introduction

Management of metastatic melanoma is extremely difficult challenge for physicians and scientists. Currently only 10% with metastatic melanoma patients survive for five years because of the lack of effective therapies [1]. There is, therefore, an emerging need to develop innovative therapies for the control of advanced metastatic melanoma.

Intracellular hyperthermia using magnetite nanoparticles (10 - 100 nm-sized, Fe_3O_4) has been shown to be effective for treating cancers in not only primary but also metastatic lesions [2-4]. Incorporated magnetite nanoparticles generate heat within the cells after exposure to AMF due to hysteresis loss [5]. In this treatment, there is not only the heat-mediated cell death but also immune reaction due to the generation of HSPs [6-15]. HSP expression induced by hyperthermia has been shown to be involved in tumor immunity, providing the basis for developing a cancer thermo-immunotherapy.

Exploitation of biological properties unique to cancer cells may also provide a novel approach to overcome difficult challenge to the melanoma treatment. Melanogenesis is inherently cytotoxic and uniquely occurs in melanocytic cells; thus, tyrosine analogs that are tyrosinase substrates can be good candidates for developing drugs to melanoma-targeting therapies [16]. N-propionyl and N-acetyl derivatives of 4S-cysteaminylphenol (NPr- and NAcCAP) were synthesized, and found to possess cytotoxic effects on *in vivo* and *in vitro* melanomas through the oxidative stress that derives from production of cytotoxic free radicals [17-21].

Based upon these rationales, we now provide evidence that melanoma-targeted *in situ* peptide vaccine immunotherapy has been successfully developed by conjugation of magnetite nanoparticles with a chemically modified melanogenesis substrate, and that a novel melanoma-targeted chemo-thermo-immunotherapy (CTI Therapy) is provided for patients suffering from advanced metastatic

melanoma.

2. Chemical Modification of Melanogenesis Substrate as a Potential Source for Development of Selective Drug Delivery System and Melanoma Toxicity

2.1. Melanogenesis Cascade in Melanoma Cells

The major advance of drug discovery for targeted therapy to cancer cells can be achieved by exploiting their unique biological property. The biological property unique to the melanocyte and melanoma cell resides the biosynthesis of melanin pigments within specific compartments, melanosomes. Melanogenesis begins with the conversion of amino acid, tyrosine to dopa and subsequently to dopaquinone in the presence of tyrosinase. This pathway is unique to all of melanocytes and melanoma cells including "amelanotic" melanoma. With the interaction of melanocyte-stimulating hormone (MSH)/ melanocortin 1 receptor (MC1R), the melanogenesis cascade begins from activation of microphthalmia transcription factor (MITF) for induction of either eu- or pheomelanin biosynthesis. Tyrosinase is the major player in this cascade. Tyrosinase is a glycoprotein and its glycosylation process is regulated by a number of molecular chaperons, including calnexin in the endoplasmic reticulum [22,23]. Vesicular transport then occurs to carry tyrosinase and its related proteins from trans-Golgi network to melanosomal compartments. In this process a significant number of transporters, such as small GTP-binding protein, adaptor proteins and PI3-kinase are involved, and early and late endosomes are closely associated with the production of these compartments. Once melanin biosynthesis is completed to conduct either eu- or pheomelanogenesis within melanosomal compartments, they will move along dendritic processes and transferred to surrounding keratinocytes in normal skin [24-26]. In metastatic melanoma cells, however, there will be no melanosome transfer inasmuch as there will be no receptor cells such as keratinocytes, and melanosomes synthesized are aggregated in autophagic vacuoles of melanoma cells. Thus a chemically modified melanogenesis substrate can be retained in melanoma cells once they are incorporated into their melanogenesis cascade, hence providing a unique drug delivery system (DDS) to melanoma cells.

2.2. Synthesis of Sulfur Analogs (Amine and Amide) of Tyrosine, Cysteaminylphenols and Their Melanocyte Toxicity

In order to utilize melanin biosynthesis pathway for developing cytocidal compounds in controlling melanoma growth, N-acetyl and N-propionyl derivatives of cysteaminylphenols (CAPs) have been synthesized [27,28] (**Figures 1**, **2**). These compounds are found to possess cytocidal effect on *in vivo* and *in vitro* melanocytes through the oxidative stress. For example, both NPrCAP and NAcCAP can selectively disintegrate follicular melanocytes after single or multiple *ip* administration to new-born or adult C57 black mice [3,29]. In the case of adult mice after repeated *ip* administration of NPrCAP, white follicles with 100% success can be seen at the site where hair follicles were plucked to stimulate new melanocyte growth and to activate tyrosinase synthesis. A single *ip* injection of NPrCAP into a new born mouse resulted in the development of silver follicles in the entire body coat. The selective disintegration of melanocytes can be seen as early as in 12 hr after a single *ip* administration. None of surrounding keratinocytes or fibroblasts showed such membrane degeneration and cell death.

A high, specific uptake of NAcCAP was seen by melanoma cell lines compared to non-melanoma cells. A melanoma-bearing mouse showed, on the whole body autoradiogram, the selective uptake and covalent binding of NAcCAP in melanoma tissues of lung and skin. The specific cytotoxicity of NPrCAP and NAcCAP was examined on various types of culture cells by MTT assay [30], showing that only melanocytic cells except HeLa possessed the low IC50. The cytotoxicity on DNA synthesis inhibition was time-dependent and irreversible on melanoma cells, but was transient on HeLa cells [21].

We also examined to what extent the melanoma growth can be blocked in both *in vitro* culture and *in vivo* lung metastasis assays by administration of NAcCAP combined with buthionine sulfoximine (BSO), which blocks the effect of anti-oxidants through reducing glutathione levels. There was a marked growth inhibition of cultured melanoma cells in the presence of BSO, indicating that the selective cytotoxicity by our NPr- and NAc-CAP is mediated by the production of cytotoxic free radicals. The *in vivo* lung metastasis experiment also showed the decreased number of lung melanoma colonies [17]. The problem was, however, that a fairly large number of amelanotic melanoma lesions were seen to grow in the lung. NPrCAP has been developed and con-

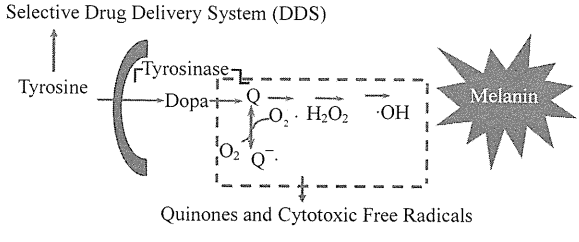

Figure 1. Exploitation of melanogenesis cascade for better management of melanoma.

	Km (μm)	Vmax (μ mole/min/mg)
Tyrosine 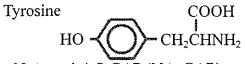	0.3	1.80
N-Acetyl-4-S-CAP (NAcCAP) H_2O_2 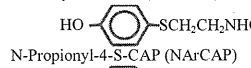	375.0	9.28
N-Propionyl-4-S-CAP (NArCAP) 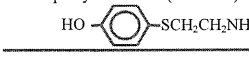	240.9	5.43

Figure 2. Synthesis and chemical structures of NAcCAP and NPrCAP and their tyrosinase kinetics.

jugated with magnetite nanoparticles in the hope of increasing the cytotoxicity and overcoming the problem.

3. Conjugation of Magnetite Nanoparticles with N-Propionyl 4S-Cysteaminylphenol, NPrCAP for Melanoma Targeted Chemo-Thermo-Immunotherapy

3.1. Synthesis for Conjugates of Magnetite Nanoparticles and NPrCAP, and Their Selective Aggregation in Melanosomal Compartments

Magnetite nanoparticles have been employed for thermotherapy in a number of cancer treatments including human gliomas and prostate cancers [31-33]. They consist of 10 - 100 nm-sized iron oxide (Fe_3O_4) with a surrounding polymer coating and become magnetized when placed in AMF [3]. We expected the combination of NPrCAP and magnetite nanoparticles to be a potential source for developing not only anti-melanoma pharmacologic but also immunogenic agent. It was expected that NPrCAP/magnetite nanoparticles complex could be selectively incorporated into melanoma cells because NPrCAP possesses a specific effect on DDS. The degradation of melanoma tissues occurs from oxidative and heat stresses by exposure of NPrCAP to tyrosinase and by exposure of magnetite nanoparticles to AMF. These two stress processes produce the synergistic or additive effect for generating tumor-infiltrating lymphocytes (TIL) that will kill melanoma cells in distant metastases (**Figure 3**).

We synthesized, in our initial study, the conjugates of NPrCAP with magnetite nanoparticles, NPrCAP/ML and NPrCAP/CML, in which NPrCAP was embedded in neutral and cationic liposomes respectively (**Figure 4**). There were, however, non-specific electrostatic interaction between cationic magneto-liposomes (NPrCAP/CML) and various non-target cells [33] as well as non-specific aggregations in neutral magneto-liposomes (NPrCAP/ML). A promising technique is the use of tumor-targeted magnetite nanoparticles, and this approach was extended by synthesizing another type of magnetite nanoparticles, NPrCAP/M and NPrCAP/PEG/M, on which NPrCAP is superficially and directly bound on the surface of magnetite nanoparticles without using liposomes. They are chemically stable, can be produced in

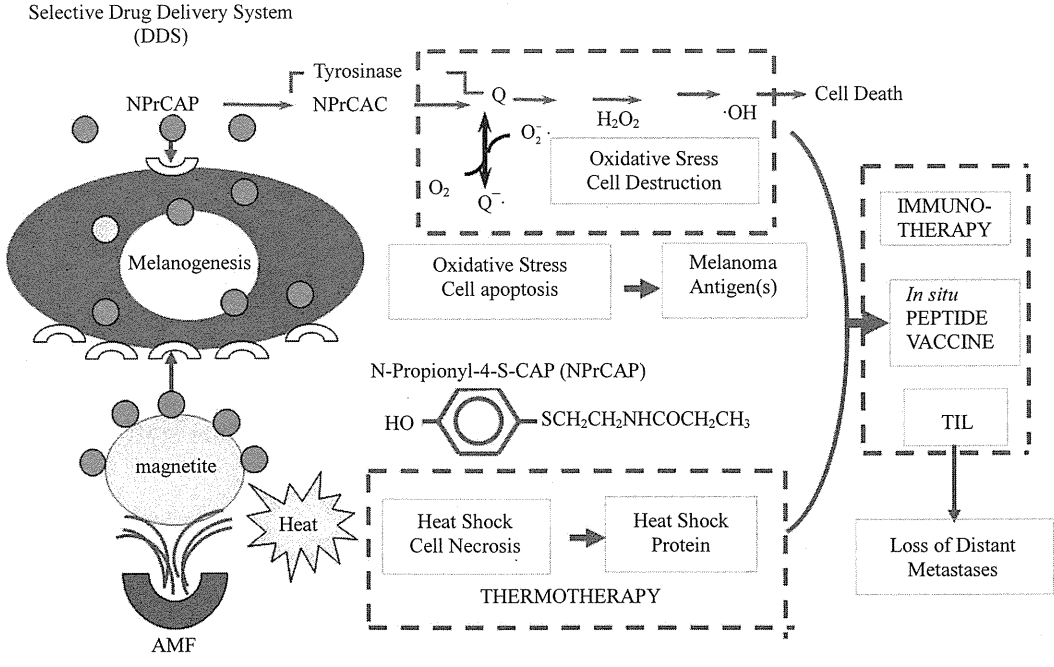

Figure 3. Strategy for melanogenesis-targeted CTI therapy by conjugates of NPrCAP and magnetite nanoparticles with AMF exposure.

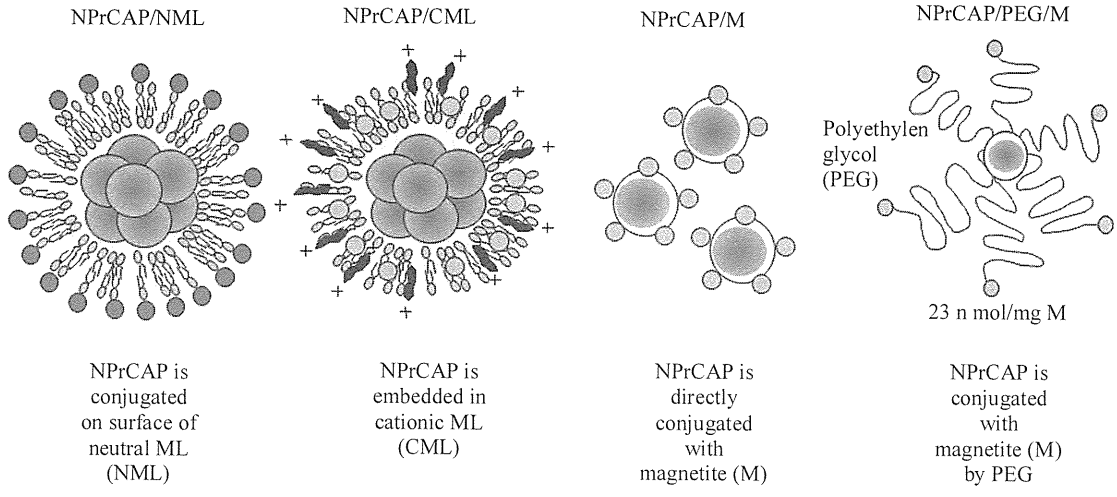

Figure 4. Conjugates of NPrCAP/magnetite nanoparticles for developing melanogenesis-targeted melanoma nanomedicine.

large quantities and may develop effective mela-noma-argeted chemotherapy (by NPrCAP) and thermo-immunotherapy (by magnetite nanoparticles with HSP), hence providing a basis for a novel CTI therapy. Most of the experiments described below were carried out by employing NPrCAP/M. A preliminary clinical trial, however, used NPrCAP/PEG/M to which polyethylene glycol (PEG) was employed to conjugate NPrCAP and magnetite nanoparticles.

In our studies, we could see that NPrCAP/M nanoparticle conjugates were selectively aggregated in melanoma cells compared to non-melanoma cells (**Figure 5(a)**). Specifically NPrCAP/M nanoparticles were found to be incorporated into and aggregated in melanosomal compartments after *ip* administration by electron microscopy (**Figure 5(b)**). After AMF exposure, there will be selective disintegration of melanoma tissues as can be seen by Berlin Blue staining [34,35] (**Figure 5(c)**). The conjugates of NPrCAP and magnetite nanoparticles will be selectively aggregated on the cell surface of melanoma cells through still unknown surface receptor and then incorporated into melanoma cells by early and late endosomes. The conjugates will then be incorporated into melanosomal compartment as the stage I melanosomes and late endosomes share common compartments, to which tyrosinase will be transported from trans-Golgi network by vesicular transport (**Figure 6**).

3.2. *In vivo* Chemo-Thermo-Immunotherapy in Mouse Melanoma by Conjugates of Magnetite Nanoparticles and Melanogenesis Substrate, NPrCAP

In this study, we employed three cell lines of B16 melanoma, *i.e.*, B16F1, B16F10 and B16-ovalbmine (OVA) cells and compared the thermotherapeutic protocols in detail by evaluating the growth of the re-challenge melanoma as well as the duration and rates of survival of melanoma bearing mice (**Figure 7**).

By employing B16F1 and F10 cells, we first evaluated the chemotherapeutic effect of NPrCAP/M with or without AMF exposure which generates heat. NPrCAP/M without heat inhibited growth of primary transplants to the same degree as did NPrCAP/M with heat, indicating that NPrCAP/M alone has a chemotherapeutic effect. However, there was a significant difference in the melanoma growth inhibition of re-challenge transplants between the groups of NPrCAP/M with and without heat. NPrCAP/M with AMF exposure showed the most significant growth inhibition in re-challenge melanoma and increased life span of the host animals, *i.e.*, almost complete rejection of re-challenge melanoma growth whereas NPrCAP/M without heat was much less, *i.e.*, 30% - 50%, indicating that NPrCAP/M with heat possesses a thermo-immunotherapeutic effect (**Figures 8(a)-(c)**).

Specifically our study indicated that the most effective thermo-immunotherapy for re-challenge B16 F1 and F10 melanoma cells can be obtained at a temperature of 43˚C for 30 min with the treatment repeated three times on every other day intervals without complete degradation of the primary melanoma (**Figure 8(b)**). Our therapeutic conditions and their effects differ from those of magnetically mediated hyperthermia on the transplanted melanomas reported previously by Suzuki *et al.* [36]. Cationic magneto-liposomes-mediated hyperthermia for B16 melanoma showed that hyperthermia at 46˚C once or twice led to regression of 40% - 90% of primary tumors and to 30% - 60% survival of mice, whereas their hyperthermia at 43˚C failed to induce regression of the secondary tumors with 0% survival of mice [36].

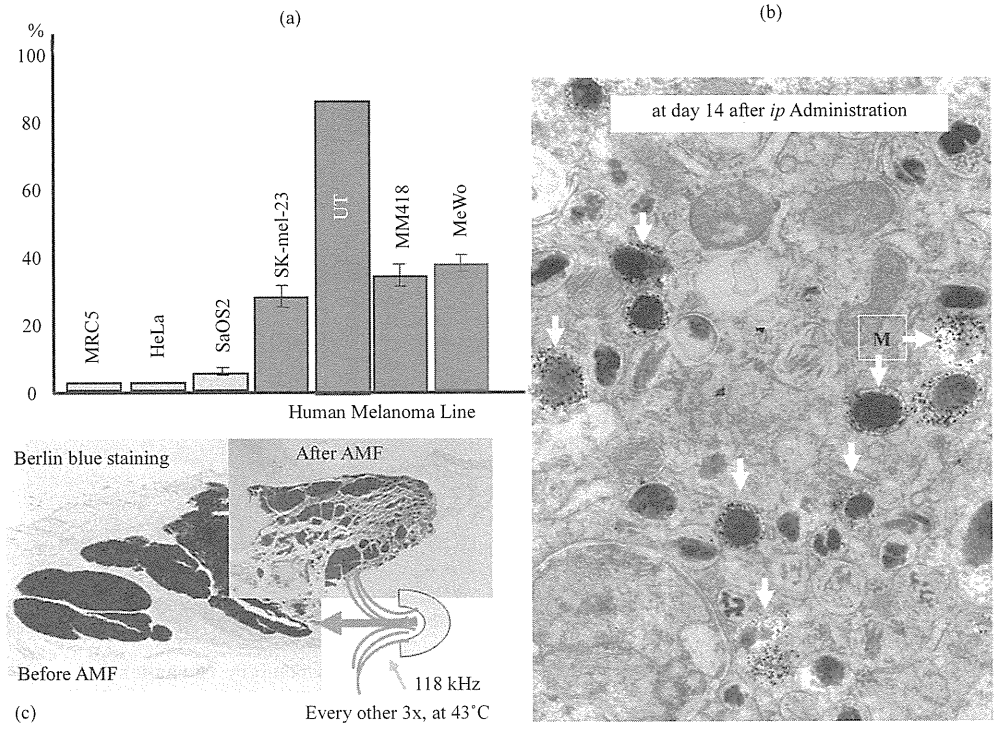

Figure 5. Selective aggregation of NPrCAP/M nanoparticles in human melanoma cell lines (a), their selective accumulation in melanosomal compartments of melanoma cells as can be seen in electron micrograph (see arrows) (b) and selective disintegration of melanoma tissues after exposure to AMF as can be seen in Berlin Blue iron staining (c).

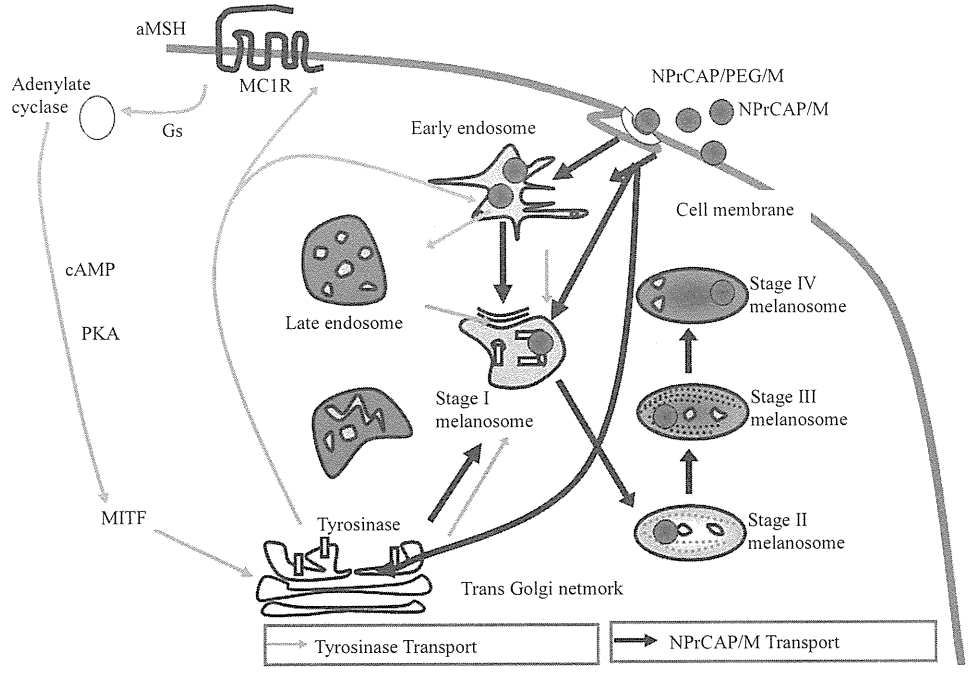

Figure 6. Selective accumulation of NPrCAP/M in melanoma cells. Conjugates of NPrCAP and magnetite nanoparticles (NPrCAP/M and NPrCAP/PEG/M) are aggregated on the cell surface of melanoma cells and incorporated into melanosomal compartments through early and late endosomes inasmuch as the stage I melanosomes derive from the specific late endosomes, to which tyrosinase will be transported from trans-Golgi network by vesicular transport.

